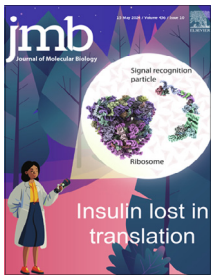

(Re)-definition of the holo- and apo-Fur direct regulons of *Helicobacter pylori*

Andrea Vannini [1,*,†], Eva Pinatel [2,†], Paolo Emidio Costantini [1], Simone Pelliciari [3], Davide Roncarati [1], Simone Puccio [4,5], Gianluca De Bellis [2], Vincenzo Scarlato [1], Clelia Peano [4,6,†] and Alberto Danielli [1,†]

*1 - **University of Bologna Department of Pharmacy and Biotechnology,** Via Selmi 3, 40126 Bologna, Italy*
*2 - **Institute of Biomedical Technologies – National Research Council,** Via Fratelli Cervi 93, 20054 Segrate (MI), Italy*
*3 - **Human Genetic Unit,** Institute of Genetic and Cancer – University of Edinburgh, Crewe Road, Edinburgh EH4 2XU, UK*
*4 - **Institute of Genetics and Biomedical Research,** UoS Milan – National Research Council, Via Manzoni 113, 20089 Rozzano (MI), Italy*
*5 - **Humanitas Clinical and Research Center,** Via Manzoni 56, 20089 Rozzano (MI), Italy*
*6 - **Human Technopole,** Via Rita Levi Montalcini 1, 20157 Milan, Italy*

***Correspondence to Andrea Vannini:** andrea.vannini5@unibo.it (A. Vannini), eva.pinatel@itb.cnr.it (E. Pinatel), paolo.costantini4@unibo.it (P.E. Costantini), simone.pelliciari@ed.ac.uk (S. Pelliciari), davide.roncarati@unibo.it (D. Roncarati), simone.puccio@humanitasresearch.it (S. Puccio), gianluca.debellis@itb.cnr.it (G. De Bellis), vincenzo.scarlato@unibo.it (V. Scarlato), clelia.peano@fht.org (C. Peano), alberto.danielli@unibo.it (A. Danielli)*
https://doi.org/10.1016/j.jmb.2024.168573
Edited by Shao Feng

Abstract

Iron homeostasis is a critical process for living organisms because this metal is an essential co-factor for fundamental biochemical activities, like energy production and detoxification, albeit its excess quickly leads to cell intoxication. The protein Fur (ferric uptake regulator) controls iron homeostasis in bacteria by switching from its apo- to holo-form as a function of the cytoplasmic level of ferrous ions, thereby modulating gene expression. The *Helicobacter pylori* HpFur protein has the rare ability to operate as a transcriptional commutator; apo- and holo-HpFur function as two different repressors with distinct DNA binding recognition properties for specific sets of target genes. Although the regulation of apo- and holo-HpFur in this bacterium has been extensively investigated, we propose a genome-wide redefinition of holo-HpFur direct regulon in *H. pylori* by integration of RNA-seq and ChIP-seq data, and a large extension of the apo-HpFur direct regulon. We show that in response to iron availability, new coding sequences, non-coding RNAs, toxin-antitoxin systems, and transcripts within open reading frames are directly regulated by apo- or holo-HpFur. These new targets and the more thorough validation and deeper characterization of those already known provide a complete and updated picture of the direct regulons of this two-faced transcriptional regulator.

Introduction

Iron is an essential micronutrient for the major human pathogen *H. pylori*, as the bacterium employs this metal as a cofactor of many redox enzymes with essential functions for the bacterium survival and for host colonization, such as detoxification (catalase, superoxide dismutase), respiration and energy production (cytochromes, hydrogenase), catabolic and anabolic reactions.[1]

On the other hand, intracellular iron could be detrimental to the bacterium, as this metal promotes formation of highly reactive oxygen species (ROS)[2] – including oxides, peroxides, and superoxides – that increase oxidative stress in the cell and directly damage the molecular components of the bacterium. Moreover, intracellular iron excess is poisonous, as this metal can substitute other cations bound to proteins, potentially compromising their proper function. Hence, *H. pylori* must tightly control iron homeostasis by carefully balancing its uptake from the environment, its use as cofactor to produce iron-employing proteins, and its storage in dedicated protein-metal complexes.

Extensive studies in this field pinpointed Fur as the key determinant of iron homeostasis in many bacteria, including *H. pylori*.[3–5] In general, this ubiquitous transcriptional regulator (TR) modulates the expression of target genes accordingly to the intracellular concentration of iron ions. The sensing mechanism is based on the property of Fur to switch from the unmetalled protein (apo-Fur) to a Fur-Fe complex (holo-Fur) according to iron levels: when iron is low, apo-Fur, which is the inactive form of the transcriptional regulator, prevails; conversely, high concentrations of iron ions convert the protein into holo-Fur, which actively binds the *cis* regulatory elements upstream the target genes, i.e. the holo-Fur boxes, and regulates gene expression.[6–8] The direct holo-Fur regulon includes genes involved in iron homeostasis, cellular metabolism, virulence, but also in transcriptional (other transcriptional regulators) and post-transcriptional (non-coding RNAs) regulation.[9–11] These regulators controlled by holo-Fur, in turn, modulate the expression of target transcripts, increasing the complexity of Fur-dependent regulation and determining the indirect holo-Fur regulon. Holo-Fur functions mostly as a repressor of transcription that employs iron as the co-repressor, while the rare examples of holo-Fur positive regulation are due to undirect regulation,[9,10] interference with other transcriptional regulators,[9,12,13] or direct activation of transcription by binding to distal Fur boxes.[13–18] It is worth noting that holo-Fur's functioning is not only modulated by iron levels, but also by levels of other transition metal ions (i.e. manganese), as well as by the oxygen concentration and pH values – as these factors change the oxidation state and availability of iron ions –, as well as by other molecules and proteins.[19]

In very few bacterial species, also apo-Fur is able to directly regulate gene expression by binding the DNA at specific sequences (apo-Fur boxes) whose consensus sequence is different from the classical Fur box.[20,21] In these bacteria, apo-Fur typically functions as transcriptional repressor, and this blockade is relieved when intracellular iron increases and converts apo-Fur into holo-Fur, i.e. apo-Fur employs iron as an inducer. Rare examples of apo-Fur positive regulation have also been reported.[17,22,23] In has been proposed that apo-Fur direct regulation relies on additional aminoacidic sequences acquired by specific orthologues of the transcriptional regulator.[24–26]

H. pylori Fur (HpFur) displays the double apo-Fur and holo-Fur regulations. Holo-HpFur is a homotetramer in solution, and its operator has a TAATAAT-n-ATTATTA consensus sequence recognizable as an inverted repeat dyad, similar to the traditional holo-Fur box. Each holo-HpFur dimer docks to a hemi-operator approaching at opposite sides of the DNA double helix by contacting residues in the DNA minor groove.[27] When multiple operators are on the same promoter, the holo-protein can form higher-order complexes that knot the DNA into compacted structures.[27] In contrast, apo-HpFur is a homodimer in solution; it recognizes its operators which harbor the TCATT-n10-TT consensus sequence which diverges from a traditional Fur box, it binds to them by inserting specific aminoacidic sequences into the major groove of DNA double helix, and it also does not form higher-order complexes on promoters that harbor multiple apo-HpFur operators.[27] Both apo- and holo-HpFur function mostly as transcriptional repressors, although few examples of positive transcriptional regulation by HpFur have been proposed.[28,29] Hence, HpFur acts as a transcriptional commutator on dedicated regulons, with holo-HpFur actively regulating holo-Fur regulon in iron-replete (fe+) conditions and apo-HpFur actively controlling the expression of apo-Fur regulon in iron-depleted (fe–) conditions.

In iron-restricted conditions, apo-HpFur reduces the storage and employment of the precious metal by directly repressing iron reservoirs (*pfr*), iron-employing enzymes as hydrogenase (*hydABCDE*), cytochromes (*cytc533*), superoxide dismutase (*sodB*, limited to certain strains), and other redox enzymes (*oorDABC*), as well as toxins (*cagA*), and other genes (*serB*, *futB*).[27,29–33,23,34,35] Conversely, when iron is too abundant, holo-HpFur reduces the import of the metal by directly repressing the expression of genes for iron importers *(fecA1*, *fecA2*, *frpB1*, *feoB*) and import-associated factors (*exbB2*, *exbD2*, *tonB*). Moreover, holo-HpFur modifies other bacterial functions by repressing a nickel-storage system (*hpn2*), the ammonia-producing aliphatic amidase (*amiE*), proteins for the biosynthesis of vitamin B2 and B6 (*pdxA*, *pdxJ*), virulence factors (*ggt*, *hofC*, *putA*), other transcriptional regulators – including *nikR* and *arsR* –, its own expression, and other genes.[28,29,36,36–43] Rare examples of transcription activation have been reported for both apo- and holo-HpFur,[23,36,44] including the anti-repression by apo-HpFur on its own promoter. In addition to the validated apo-HpFur and holo-HpFur regulons, -omic approaches have pinpointed many other HpFur-regulated genes in response to iron levels,[33,45] as well as many genomic sites bound in vivo by HpFur in either fe+ or fe– conditions,[28]

indicating extensive HpFur direct and indirect regulons.

Given the complexity and extent of the HpFur regulons, in this work we aim to unravel the direct regulons in both iron-replete (fe+) and depleted (fe−) conditions through a comprehensive genome-wide analysis (see the Graphical abstract).

Results

Transcriptional analysis of fe+ and fe− dependent transcriptional responses

To identify genes transcriptionally regulated by HpFur in response to iron availability, we analyzed the transcriptome of *H. pylori* in iron-replete (fe+) and −depleted (fe−) conditions by RNA sequencing. For the assay, we employed a wild type (wt) and an isogenic *fur* deletion mutant (Δ*fur)* to discriminate HpFur-dependent transcriptional alterations from those driven *per se* by changes in iron concentration. Liquid cultures of wt and Δ*fur* strains were grown to the mid-late exponential phase, treated with an excess of iron (fe+) or with an iron chelator (fe−) for 20 min, and the purified RNAs were used to generate cDNA libraries that were sequenced and analyzed (refer to Methods, Supplementary Table 1, and Figure S1A for details). The comparison between fe+ and fe− conditions revealed the presence of 165 iron-dependent differentially expressed genes (iDEGs) in the wt strain and of 26 genes in the Δ*fur* strain (Figure 1A; more details in Supplementary Table 2, Figure S1B and S1C). Just 11 iDEGs were listed for both wt and Δ*fur* strains (Figure 1A, dark green and dark red circles), and 3 of them showed relevant differences in iron responses between the two strains, indicating a possible role of HpFur in their regulation. Hence, in the experimental conditions tested, HpFur appears to contribute to most of the iron-dependent transcriptional responses of *H. pylori* (92%, Figure 1A).

Prompted by this observation, we decided to isolate HpFur-dependent iron responses not just intersecting iDEG lists obtained from the two strains, but subtracting the variations detected in Δ*fur* strain from those measured in the wt strain, i.e. calculating log2FC (wt/Δ*fur*). According to the selected threshold values (see Methods and legend to Figure 1B), we ended up with a list of 149 HpFur-dependent differentially expressed genes in response to iron variations – the fDEGs (Figure 1B), that were mostly already listed in wt iDEGs (129/149). A set of 52 fDEGs were induced by iron (Figure 1B red and Supplementary Table 3) while 97 fDEGs were repressed by iron (Figure 1B green and Supplementary Table 4); these lists of fDEGs formed the basis for all subsequent analyses. To discriminate between HpFur repression and activation, the fDEGs were further classified comparing their expression levels in the wt and Δ*fur* strain in the fe+ and fe− conditions. Of the fDEGs repressed by iron, 33 genes resulted more abundant in the Δ*fur* than in the wt strain under the fe+ condition, indicating that they are repressed by HpFur in the presence of high amounts of iron (holo-HpFur repression, Figure 1C cyan); 48 genes were less abundant in the Δ*fur* strain than the wt in the fe−, indicating that they are induced by HpFur when iron levels are low (apo-HpFur activation, Figure 1C pink); the remaining 16 transcripts showed variations ascribed to both classes of regulations (mixed holo-HpFur repression & apo-HpFur activation, Figure 1C grey). Conversely, of the fDEGs induced by iron, 46 genes were more abundant in the Δ*fur* strain than the wt in the fe− condition, indicating that they are repressed by HpFur when the iron is low (apo-HpFur repression, Figure 1C orange). The remaining 6 genes were less abundant in the Δ*fur* strain than the wt in fe+, indicating that they are induced by HpFur when iron levels are high (holo-HpFur activation, Figure 1C black). Genes representative for the first 4 major classes of HpFur-dependent regulation were selected for validation by qRT-PCR (Figure 1D and Figure S1D).

Globally, the RNA-seq approach allowed the definition of 5 distinct HpFur-dependent classes of regulation: 1) holo-HpFur repression (22%), 2) apo-HpFur repression (31%), 3) apo-HpFur activation (32%), 4) holo-HpFur repression & apo-HpFur activation (11%), and 5) holo-HpFur activation (4%).

HpFur regulation in response to iron mainly involves whole operons

The lists of fDEGs were then clustered into transcriptional units (TUs) by DOOR operon prediction, followed by manual revision of the results. Analysis of the fDEGs induced by iron identified 32 apo-HpFur repressed TUs (Figure 1C orange circles and Supplementary Table 3, orange background) and 5 holo-HpFur activated TUs (Figure 1C black circles and Supplementary Table 3, white background). Significantly, the apo-HpFur repressed group included most of the genes already known to be directly repressed by apo-HpFur, including *pfr, cytc553*, *hydABCDE*, and *oorDABC*.[27,29–33,23,34,35] In addition to the genes significantly deregulated in the RNA-seq assay (Supplementary Table 3, text colored in red/-green and highlighted in bold), most genes within each TU showed a similar trend for iron- and HpFur-dependent regulation, although under the selected threshold (Supplementary Table 3, text colored in red/green non-bold). Thus, as expected, regulation of the TUs likely occurs at the level of their promoters. In contrast, a fraction of apo-HpFur repressed TUs (Supplementary Table 3, cells highlighted in dark orange) contained genes

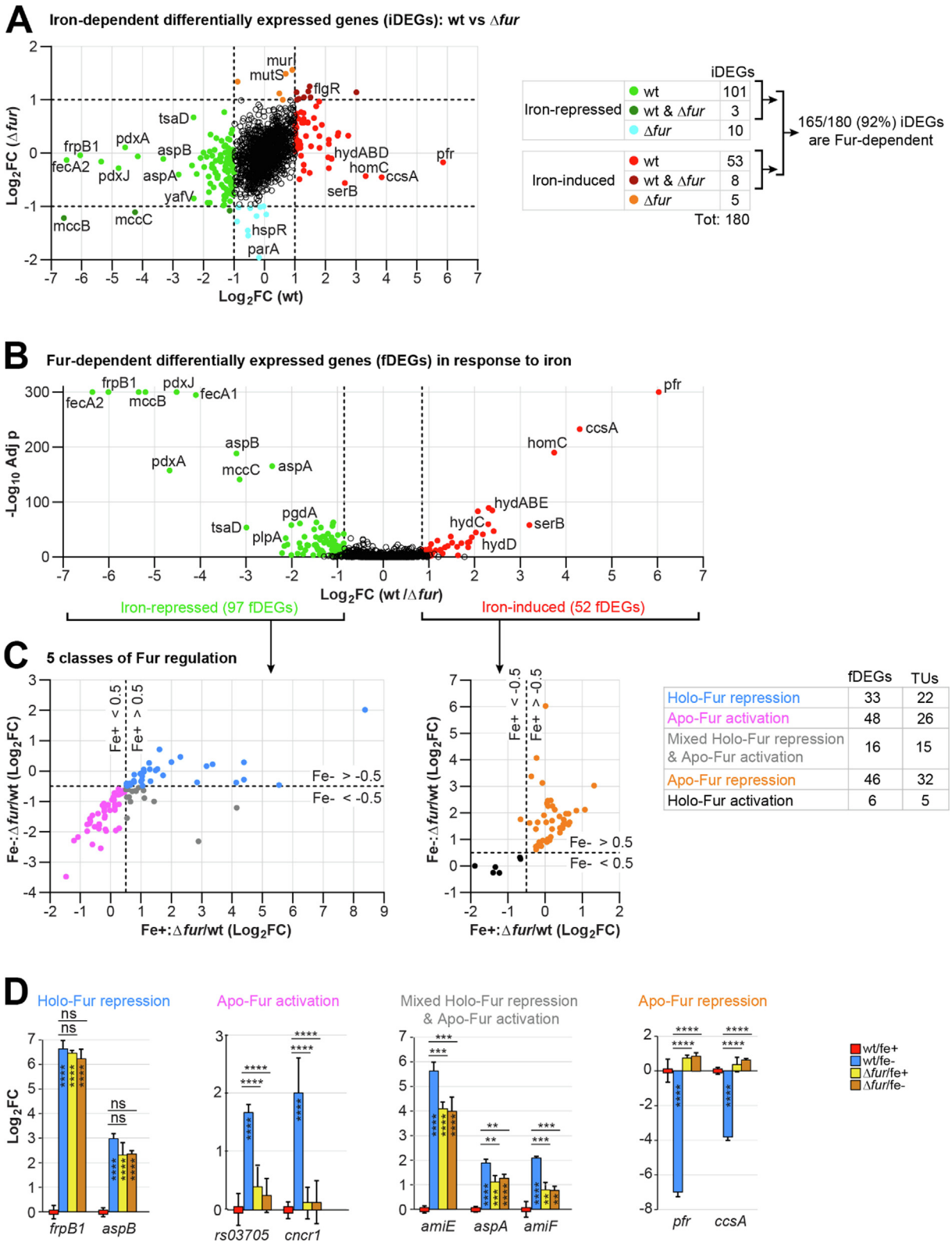
A
Iron-dependent differentially expressed genes (iDEGs): wt vs Δfur
Log2FC (Δfur)
Log2FC (wt)
murI
mutS
flgR
tsaD
frpB1
pdxA
aspB
fecA2
pdxJ
aspA
yafV
hydABD
homC
ccsA
pfr
serB
mccB
mccC
hspR
parA
iDEGs
Iron-repressed
wt 101
wt & Δfur 3
Δfur 10
Iron-induced
wt 53
wt & Δfur 8
Δfur 5
Tot: 180
165/180 (92%) iDEGs are Fur-dependent
B
Fur-dependent differentially expressed genes (fDEGs) in response to iron
-Log10 Adj p
Log2FC (wt /Δfur)
frpB1
pdxJ
fecA1
fecA2
mccB
pfr
ccsA
homC
aspB
pdxA
mccC
aspA
hydABE
pgdA
hydC
serB
tsaD
plpA
hydD
Iron-repressed (97 fDEGs)
Iron-induced (52 fDEGs)
C
5 classes of Fur regulation
Fe-:Δfur/wt (Log2FC)
Fe+:Δfur/wt (Log2FC)
Fe+ < 0.5
Fe+ > 0.5
Fe- > -0.5
Fe- < -0.5
Fe+ < -0.5
Fe+ > -0.5
Fe- > 0.5
Fe- < 0.5
fDEGs TUs
Holo-Fur repression 33 22
Apo-Fur activation 48 26
Mixed Holo-Fur repression & Apo-Fur activation 16 15
Apo-Fur repression 46 32
Holo-Fur activation 6 5
D
Holo-Fur repression
Apo-Fur activation
Mixed Holo-Fur repression & Apo-Fur activation
Apo-Fur repression
Log2FC
ns
frpB1
aspB
rs03705
cncr1
amiE
aspA
amiF
pfr
ccsA
wt/fe+
wt/fe-
Δfur/fe+
Δfur/fe-

not regulated in response to iron (in black) clustered at the beginning or end of the TUs.

Operon analysis of the fDEGs repressed by iron identified 22 holo-HpFur repressed TUs (Figure 1C cyan circles and Supplementary Table 4, cyan background), 26 apo-HpFur activated TUs (Figure 1C pink circles and Supplementary Table 4, pink background), and 15 TUs which showed mixed holo-HpFur repression & apo-HpFur activation (Figure 1C grey circles and Supplementary Table 4, grey background). Accordingly, lists of holo-HpFur repression and of the mixed holo-HpFur repression & apo-HpFur activation included most of the genes known to be directly repressed by HpFur in iron-replete conditions (*fecA1, fecA2, frpB1, arsR*, *pdxJ*, *ggt*, and *amiE*).[28,29,40–43] In the TUs of the above-described 3 groups, the majority of the genes were regulated (Supplementary Table 4, text colored in red/green and highlighted in bold) or showed the same trend of regulation (Supplementary Table 4, text colored in red/green non-bold), indicating that HpFur-dependent direct or indirect regulations in response to iron occur at the operon promoters.

The TUs in which the variations of transcript levels are limited to the 5′ or 3′ region of the operon may result from the regulation of an internal promoter, a post-transcriptional regulation by factors regulated by HpFur, polar effects of transcription and degradation that may alter the kinetic of mRNA variations in the different positions of the transcript (i.e., regulation at the 3′ end of the transcript may be detectable at later time points), or could be involved in still undetermined regulatory mechanisms.

Identification of the genomic regions bound by HpFur

To define the DNA regions bound in vivo by HpFur in holo (fe+) and apo (fe−) conditions, we proceeded with a ChIP-sequencing experiment. Similarly to the RNA-seq assays, wt and Δ*fur H. pylori* strains were grown to the mid-late exponential phase, exposed to fe+ or fe− conditions for 20 min, and then treated with 1% formaldehyde for the crosslinking of the proteins bound to the DNA. HpFur-bound chromatin was immunoprecipitated (IP) using a specific anti-HpFur polyclonal antibody (Figure S2A), and the recovered DNA fragments were subject to deep sequencing. At least 2.3 million raw reads were obtained for each IP sample and biological replicate (Bioproject: PRJNA313048, see Supplementary Table 1 for the mapping quality controls). Holo- and apo-HpFur peaks were identified by comparing the wt/fe+ or wt/fe− conditions with the Δ*fur*/fe+ sample, employed as the experiment's negative control (background). The most consistent and reproducible peaks between the two independent biological replicates produced for each condition were selected by measuring the irreproducible discovery rate (IDR), which resulted in the identification of 140 peaks in the wt/fe+ condition (holo-HpFur peaks) and 48 peaks in the wt/fe− condition (apo-HpFur peaks). All samples and replicates met the ENCODE parameters of reproducibility (See Supplementary Table 1), although wt/fe− replicates were borderline.

Figure 1. Distinct classes of HpFur-dependent regulation revealed by RNA-sequencing analysis. (A) RNA-seq analysis of iron-dependent transcriptional responses (iDEGs). log2FC values of iron treated (fe+) vs iron deprived (fe−) samples are reported for wt (x-axis) and Δ*fur* (y-axis) genotypes. Transcripts repressed (log2FC $\leq$ -1; adj $p < 0.01$) after iron addition in the wt (green), Δ*fur* (azure), or both strains (dark green); transcripts induced (log2FC $\geq$ 1; adj $p < 0.01$) after iron addition in the wt (red), Δ*fur* (orange), or both strains (dark red); empty black circles correspond to non-differential genes. The number of iDEGs in the different categories is shown in the right panel. More details in Figure S1 and Supplementary Tables 1 and 2. The adj p indicates BH (Benjamini-Hochberg) adjusted p-value. (B) Identification of HpFur-dependent iron responses (fDEGs). Volcano plot of the wt/Δ*fur* ratios vs adj p (wt): repressed (green), induced (red), or non-differential (empty black) transcripts after iron addition (log2FC (wt/Δ*fur*) $\geq$ |0.85|; log2FC (wt) $\geq$ |0.65|; adj p (wt) < 0.01). The numbers of iron-repressed and -induced fDEGs are indicated below the graph. (C) Iron-repressed and -induced fDEGs were further classified according to the wt vs Δ*fur* expression ratio in iron depleted (fe−) and replete (fe+) conditions. 5 classes of HpFur regulation were determined: holo-HpFur repression (Δ*fur* > wt in fe+ condition; cyan), apo-HpFur activation (Δ*fur* < wt in fe− condition; pink), mixed holo-HpFur repression & apo-HpFur activation (Δ*fur* > wt in fe+ condition and Δ*fur* < wt in fe− condition; grey), apo-HpFur repression (Δ*fur* > wt in fe− condition; orange) or holo-HpFur activation (Δ*fur* < wt in fe+ condition; black). The fDEGs were grouped into transcriptional units (TUs), and the number of fDEGs and TUs in the 5 classes of HpFur regulation is reported in the right panel. More details in Supplementary Tables 3 and 4. (D) Validation of fDEGs representative of the different classes of HpFur regulation by qRT-PCR. Data were normalized on 16S RNA and reported as log2 fold changes relative to the wt/fe+ condition that was set to the value of 0 (mean values of at least three biological replicates ± SD). Statistical significance was calculated using ordinary one-way ANOVA test (*$P < 0.05$; **$P < 0.01$; ***$P < 0.001$; ****$P < 0.0001$) after the Shapiro-Wilk and Bartlett's tests to check the normal distribution of the results and the equality of variances, respectively.

The holo- and apo-HpFur peaks were classified according to their positions relative to the transcription start sites (TSS). Of the 140 holo-HpFur peaks, 22 were classified "promoter" peaks as they mapped within promoter regions, 112 peaks fall within coding regions and were defined as "inside" peaks, and 6 were called "intergenic" peaks as they mapped to intergenic regions outside the core promoter of TUs (Figure 2A and Supplementary Table 5).

Re-definition of holo-HpFur directly repressed regulon by transcriptomic and ChIP-seq data integration

Each TUs that allowed the classification of holo-HpFur peaks (see the previous paragraph) was associated to the corresponding peak: 25 TUs were associated to the "promoter" peaks (of the 22 peaks, 3 mapped on divergent promoters), 112 TUs were associated to the "inside" peaks, and 12 TUs were associated to the "intergenic" peaks as

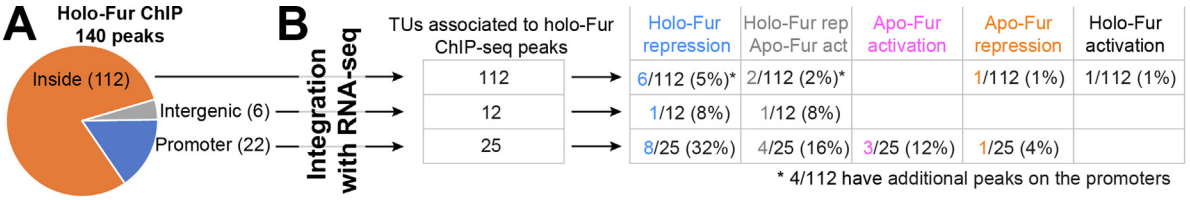

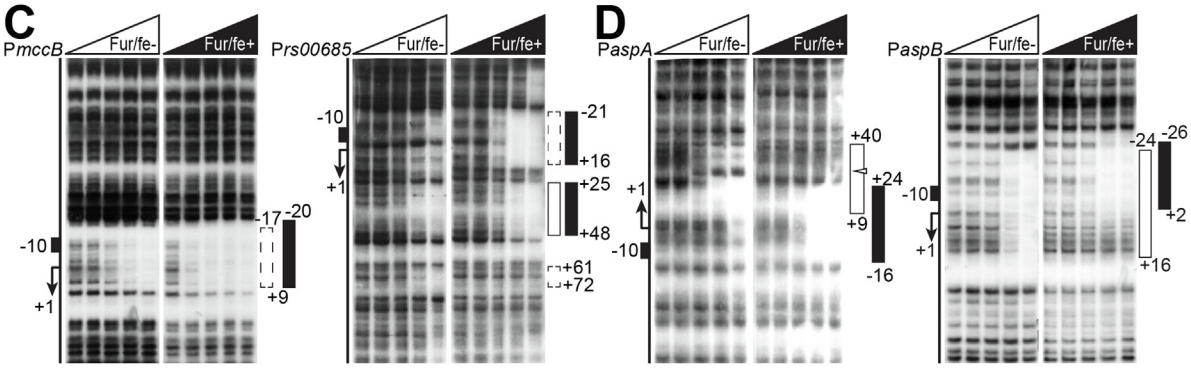

Promoter	Sequence	Strand	Score
mccB	ATTATAATTATTGTTATTAT	-	23.4
amiE	ATAATAATTAAAGTTTTCAT	+	22.3
fecA2 (OP2)	ATTTTAATAATTATTTTTAT	-	22.0
fur (OP1)	AAAATAATAATGAGTTTTAT	-	21.7
ribBA	AAAGTAATAATCGTTATTAA	-	20.5
frpB1	GTTTTAATAATAATTATCAT	+	19.8
fecA1	AAACTAATAATGGTTATTAT	-	19.0
nc2090	ATTAAAACTATGATTACTAA	-	15.3
nc4590	ATTAAAACTATGATTACTAA	+	15.3
rs05100	AAAATAATGATAATAATCAT	-	15.3
nikR	TTTGT.ATTATAATTGTTAA	-	14.7
exbB1	ATTGTAATTATTAGCTTAAT	+	14.7
fur (OP2)	ATAAT.ATTCTAGTTATAAA	-	12.6
rs00685	TTTATAATTATCGTAAGCAT	+	12.5
ggt	GTTATAATAACGATTATTGT	-	11.3
nc0040	AAGGT.ATAATAGTTTCCAA	-	11.2
arsR (OP1)	ACTATGATAATGTTTTGAAT	-	11.0
nc8160	AAAGT.ATAATGTCTTCCAA	-	10.4
aspB	ATTAGAATTAAAATCTTTTT	+	9.92
ceuE2	TTTGTGAAAAAAAGTTTCAT	-	9.83
amiF	GCAATAATTGTTATTGTTAT	+	9.01
arsR (OP2)	TTAAAAAATAAGACTTTAAT	-	8.76
fecA2 (OP1)	AAATG.AGAAAGGTTATCAT	-	8.04
arsR (OP3)	AAAGT..TAATCGTTTTTAA	-	7.16
aspA	ATAGCTAGAATATTTTTCAA	+	6.69

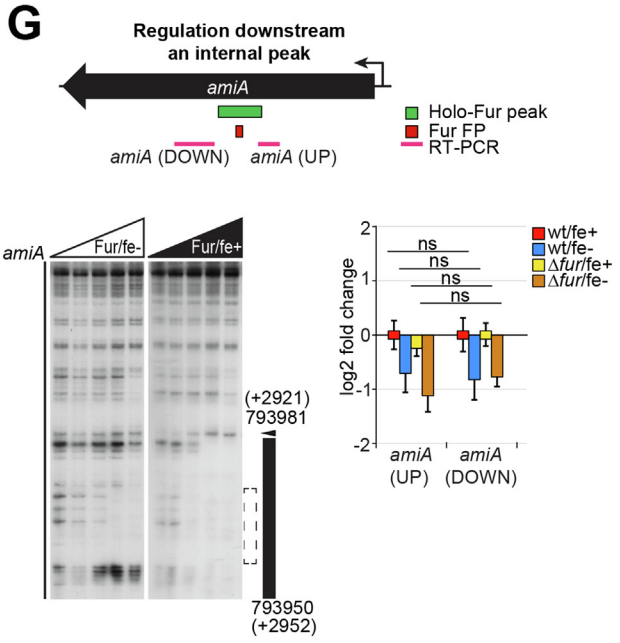

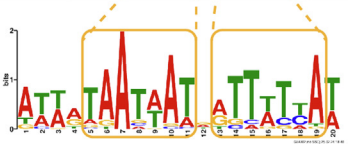

we considered both the nearest TUs upstream and downstream the peaks (Figure 2B and Supplementary Table 5). To determine if the binding of holo-HpFur to the DNA mapped in the holo-HpFur ChIP-seq experiment could correlate to transcriptional regulation, ChIP-seq data were integrated with the TUs containing fDEGs (Figure 2B and Supplementary Table 5). As for the 25 TUs associated to "promoter" peaks, 15 (60%) were iron-repressed: 8 TUs were holo-HpFur repressed (cyan), 3 TUs were apo-HpFur activated (pink), and 4 TUs belonged to the mixed holo-HpFur repression & apo-HpFur activation group (grey). In addition, a holo-HpFur peak encompassed the promoter of the *pfr*, known to be repressed by apo-HpFur (orange). Of the 112 TUs associated to "inside" peaks, only 10 (9%) were regulated by HpFur in response to iron, including 4 TUs that were already associated to "promoter" peaks (Figure 2B and Supplementary Table 5). Of the 12 TUs associated to "intergenic" peaks, only 2 TUs belonged to the groups holo-HpFur repression and mixed holo-HpFur repression & apo-HpFur activation.

Globally, the association between the holo-HpFur ChIP-seq peaks, their nearest TUs, and the HpFur-dependent regulation of these TUs in response to iron as determined in the RNA-seq data analysis resulted in an enrichment bias towards the promoter regions and towards holo-HpFur repression or mixed holo-HpFur repression & apo-HpFur activation (Supplementary Table 5). Some of these TUs contain gene known to be directly targeted and repressed by holo-HpFur: *frpB1, fecA2, pdxJ, fecA1*, *ggt, arsR,* and *hpn2*.[27,29,33,39–41,46] In addition, 5 new TUs appeared to be directly targeted by holo-HpFur on their promoters, resulting in holo-HpFur repression: *ribBA*, *amiF*, *mccB-mccC*, *yafV*, and *rs00685*.

The binding of HpFur to the promoters of these latter genes was validated by DNase I footprinting assay (Figure 2C and Figure S2B). In all tested promoters, one or more areas of protection from DNase I digestion appeared in the fe+ condition, indicating a specific high-affinity interaction between holo-HpFur and each of the tested DNA probes in the range of 1.7–5.6 nM of the holo-HpFur tetramer. In the fe− condition, HpFur partially maintained its ability to interact with the probes, showing a reduced protection area at high concentrations of the HpFur protein (in the range of 11–34 nM of the apo-HpFur dimer), indicating a lower affinity of the protein to the DNA. The analysis was performed also promoter of *ggt*, a

Figure 2. Deciphering the holo-HpFur directly repressed regulon: integrating holo-HpFur ChIP-seq and RNA-seq data. (A) Holo-HpFur ChIP-seq peaks predicted by Homer2 and complying the IDR parameters were classified as "inside", "intergenic", and "promoter" according to their genomic locations and distances from TSS. (B) TUs were associated to the holo-HpFur ChIP-seq peaks: 1–2 TUs for each "promoter" peak (1 for the monodirectional promoters, 2 for the bidirectional promoters), 1 TU for each "inside" peak, and 2 TUs for each "intergenic" peak. These TUs were further classified according to the HpFur's classes of regulation, as determined in RNA-sequencing. (C) Validation of holo-HpFur "promoter" binding sites by DNase I footprinting assay. Radiolabeled DNA probes encompassing the promoters of *mccB* (HPG27 plasmid, specific of G27 strain) or *rs00685* (HP0135 in strain 26695) were mixed with increasing amounts of HpFur, in the presence of iron chelator (150 μM 2,2′-Dipyridyl, left side of panel) or iron (150 μM $(NH_4)_2Fe(SO_4)_2$, right side of panel), before DNase I cleavage. The concentrations of the apo-HpFur dimer were 0, 3.4, 11.2, 34, and 112 nM; those of the holo-HpFur tetramer were 0, 1.7, 5.6, 17, and 56 nM. On the right of each autoradiographic film, DNaseI-protected regions in fe− (dotted empty box) and fe+ (black box) conditions and their position with respect to the TSS are shown. On the left, a schematic representation of the promoter is provided, with the TSS (+1, bended arrow) and the −10 region (black box). (D) Validation by DNase I footprinting assay of additional holo-HpFur "promoter" binding sites manually identified among the holo-HpFur ChIP-seq peaks obtained with more relaxed parameters of analysis. The radiolabeled probes encompassing *aspA* (HP0649) and *aspB* (HP0672) promoters were employed. Experimental conditions, numbers, and symbols as in panel C. (E) List of the DNA sequences aligned by GLAM2 to generate the consensus sequence for holo-HpFur repression. All the DNA sequences bound by holo-HpFur in DNaseI footprinting assays (in this work and those known in the literature) were employed for the analysis. The DNA strand in which the sequences are located (+and −) and the score resulting from realigning each sequence to the consensus are reported. (F) Weblogo of the consensus sequence for holo-HpFur repression derived from the analysis in panel E. (G) Characterization of an "inside" HpFur binding site mapping within the *amiA* CDS. The *amiA* genomic locus is depicted in the left panel, along with the position of holo-HpFur peak (green), of the protected region in DNaseI footprinting assay (red), and of the qRT-PCR amplicons (pink). In the bottom-left panel, validation of holo-HpFur binding on the DNA by DNaseI footprinting assay; experimental conditions, numbers, and symbols as in panel C. In the bottom-right panel, qRT-PCR analysis of *amiA* transcript levels upstream (*amiA*-UP) and downstream (*amiA*-DOWN) the HpFur binding site. Experimental condition and visualization of the results as in Fig 1. Transcription levels in UP and DOWN positions were compared for each condition by *t*-test after Shapiro-Wilk and F tests, resulting in no significant difference in any of the comparisons (ns, $P > 0.05$).

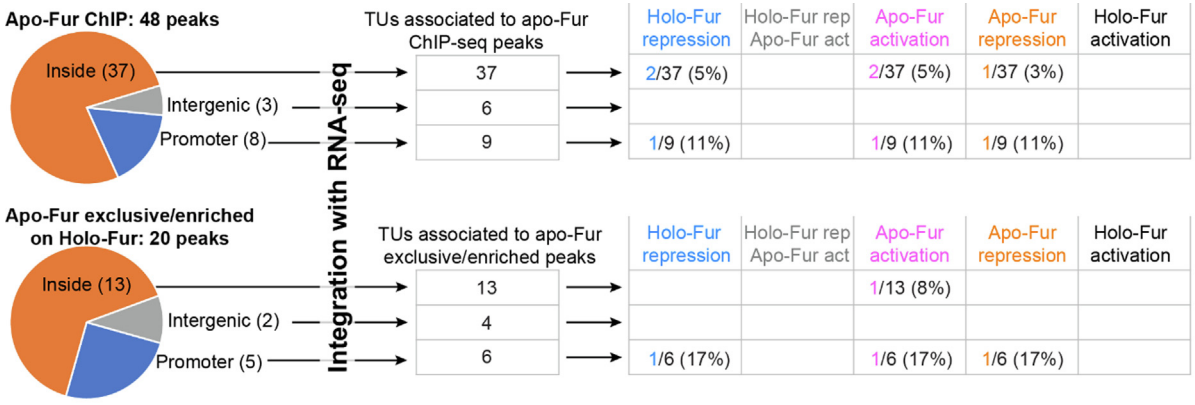

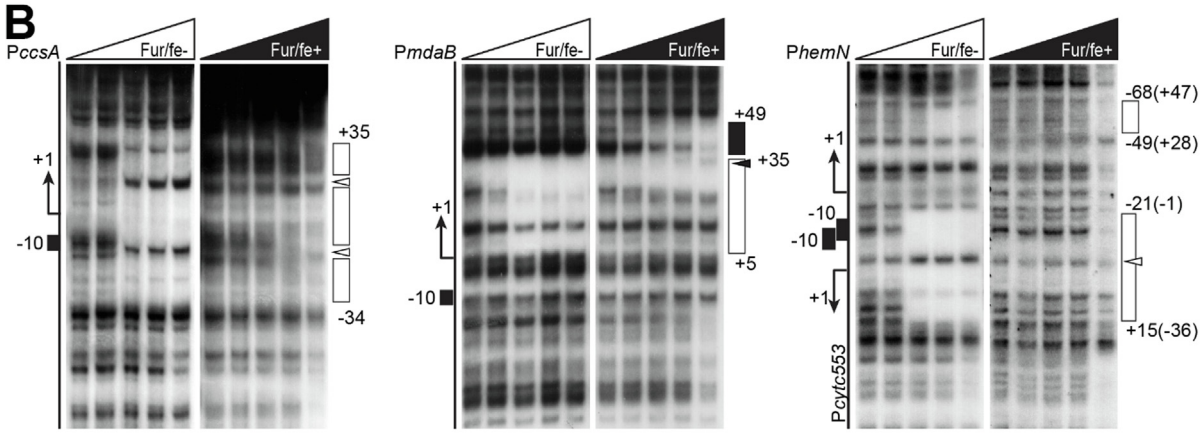

C

Promoter	Sequence	Strand	Score
pfr (OP2)	TCTCATTTTTTGCAAGTTTTTAAAA	+	23.6
mdaB	TTTCATTTTGTTT.CCTTTTTTAATA	-	22.7
ccsA	TCTTATTATAACCACCATTTTAAAA	-	21.9
hydA	TTTCATTATCTT.AACATAATAAAA	-	21.4
cytc553/hemN	TATCATTTTAAG.ATCATTTTGATA	+	19.8
homC	TCTTATTATAAT.ACATTTTTGAGA	-	18.7
pfr (OP3)	TCTCATTAAATAGATTTTTATGATA	+	18.6
pfr (OP1)	TTTCATTATCATTTATGCTATAATT	+	12.6

E

Promoter	From	To	Sequence	EMSA
rs05875	-5	+12	TTTTTATTATCAATCCTACTTTCCTA	YES
ansB (OP 1)	-32	-16	ATTTTATTTTTAACGATGTTTTACTA	YES
ansB (OP 2)	+17	+33	TCTCATTATGGACCACCTTTTGAAA	
dld	-16	+1	AATCATTGTAACATAACCTTACTTT	YES
vlpC	-53	-37	AGTCATTTTGCGAATCTTTTTGAGT	YES
uvrA	-6	+11	GATCATTATTCAAGGGGCTAGGGAA	NT
horl	+12	+28	ATTTTATTTTATACGATATTAAGGAG	NT
rs07455	+6	+22	CTTTTATTCATGGGAAAATTAAAGAG	NT

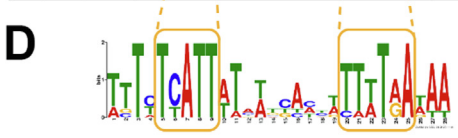

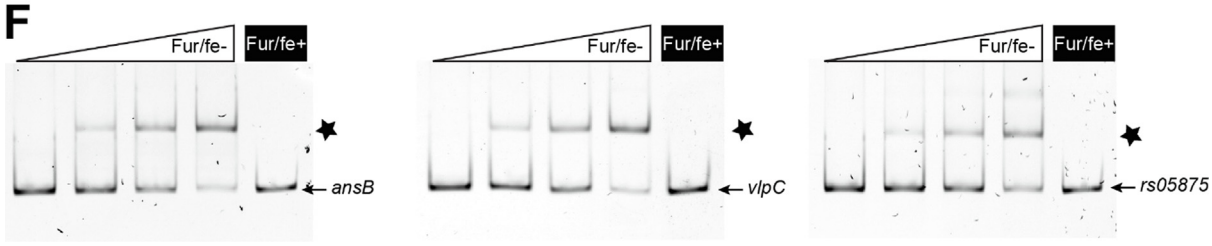

gene known to be directly targeted and regulated by holo-HpFur to precisely map the binding sites (Figure S2B). Hence, for all these promoters, HpFur directly binds to DNA in the presence of iron (holo-HpFur) and represses the expression of the downstream genes. The *ribBA*, *amiF*, *mccB-mccC*, *yafV*, and *rs00685* TUs are new members of the holo-HpFur directly repressed regulon.

Manual revision of the holo-HpFur ChIP-seq tracks guided by the lists of TUs repressed by holo-HpFur allowed the identification of other promoter regions bound in vivo by holo-HpFur and associated to holo-HpFur repression. The bindings of HpFur to the promoters of the *amiE*, *aspA-rs03170*, and *aspB-rs03275* TUs were validated by DNase I footprinting assays (Figure 2D and Figure S2C), further extending the holo-HpFur directly repressed regulon.

All the DNA sequences protected by holo-HpFur in the DNase I footprinting assays as determined in this work (see also next chapters) or from literature,[39–41,47] and that resulted repressed by holo-HpFur in vivo were aligned (Figure 2E) to generate the consensus sequence for holo-HpFur direct repression (Figure 2F).

The vast majority of holo-HpFur "inside" peaks are not associated with the regulation of transcription (Figure 2B). Some of the few exceptions are genes that are directly regulated by HpFur through an additional binding site overlapping their promoters, as it is likely the case for the "inside" peaks within *fecA1*, *frpB1*, *mccB*, and *tsaD* promoters (see Supplementary Table 5). However, all the "inside" peaks that were selected for validation by DNase I footprinting assay confirmed holo-HpFur binding on the DNA (Figure 2G, Figure S2D, as well as the validation of HpFur binding on peak_2, peak_3, peak_20, and peak_33 of Supplementary Table 5 that will be part of a different article). Interestingly, the RNA-seq profiles of genes with holo-HpFur "inside" peaks did not show any iron-induced variations of transcript levels downstream of the HpFur binding site. This observation was validated for the *amiA* mRNA by qRT-PCR (Figure 2G) by comparing the transcript levels upstream and downstream of the HpFur binding site. No differences in transcript levels were detected, indicating an absence of iron-dependent regulation by HpFur on this "internal" binding site.

Partial definition of the apo-HpFur directly repressed regulon

Of the 48 apo-HpFur peaks, 8 were classified as "promoter" peaks, 37 as "inside", and 3 as "intergenic" peaks (Figure 3A and Supplementary Table 6). Proceeding as described in the previous chapter, we associated the apo-HpFur peaks to the corresponding TUs (Figure 3B and Supplementary Table 6). Surprisingly, the "promoter" TUs included only two of the genes known to be directly regulated by apo-HpFur (*pfr* and *fur* itself[27,31,36]), while others were missing, including *cytc553*, *hydABCDE*, *cagA*, and *oorDABC*.[23,34,35] The observation that holo-HpFur repressed *fecA2* was retrieved among the apo-

Figure 3. Deciphering the apo-HpFur directly repressed regulon: integration of RNA-seq, Footprinting, and EMSA analysis. (A) ChIP-seq peaks of apo-HpFur predicted by Homer2 and complying the IDR parameters were classified as "inside", "intergenic", and "promoter" according to their genomic locations and distances from TSSs. TUs associated with the peaks (see details in Figure 2 – panel A) were classified according to HpFur's classes of regulation (top panel). The analysis was also restricted to the peaks exclusive to apo-HpFur or enriched in apo-HpFur with respect to holo-HpFur immunoprecipitation (lower panel; more details in Supplementary Table 6). (B) Determination of HpFur binding sites on the promoters of TUs of the apo-HpFur repression class of regulation by DNase I footprinting assay. Radiolabeled probes encompassing the promoters of *ccsA* (HP1461 in strain 26695), *mdaB* (HP0630), and the bidirectional *cytc553* (HP1227) – *hemN* (HP1226) promoters were used for the assay. Experimental conditions, numbers, and symbols as in Figure 2. (C) List of the DNA sequences aligned by GLAM2 to generate the consensus sequence for apo-HpFur repression. All the DNA sequences bound by apo-HpFur in DNaseI footprinting assays (in this work and those known in the literature) were employed for the analysis, with the exception of the *oorD* promoter,[23] in which the boundaries of the apo-HpFur binding site were determined at too low resolution for the analysis. The relative orientation of each sequence with respect to the associated TSS (+and –) and the score resulting from realigning each sequence to the consensus are reported. (D) Weblogo of the consensus sequence for holo-HpFur repression derived from the analysis in panel C. (E) Identification of the consensus sequence for apo-HpFur repression within the promoters of other TUs repressed by apo-HpFur. Subsequent validation of direct binding of apo-HpFur on these promoters is reported on the right (EMSA). (F) Visualization by EMSA assay of direct binding of apo-HpFur to some of the promoters identified in the analysis shown in panel E. DNA probes encompassing the promoter regions of *ansB* (HP0723), *vlpC* (HP0922), and *rs05875* (HP1181) promoters were incubated with increasing amounts (0, 2.1, 4.9, and 11.2 nM) of apo-HpFur dimer in the presence of iron chelator (150 μM 2,2′-Dipyridyl) or 11.2 nM of holo-HpFur tetramer in the presence of iron (150 μM $(NH_4)_2Fe(SO_4)_2$). Samples were resolved on a 6% acrylamide gel, free DNA probes (arrow) and complexes (star) between apo-HpFur and DNA are visible.

HpFur "promoter" TU suggested a partial overlap of the apo- and holo-HpFur peak lists. Indeed, 42 out of the 48 apo-HpFur peaks were shared with holo-HpFur, and only 6 peaks were specific for apo-HpFur (Supplementary Table 6). The fold enrichment of apo- and holo-HpFur shared peaks showed that only 14 of the 42 shared peaks were more enriched in the fe− condition with respect to the fe + (Supplementary Table 6). Among the 14 apo-HpFur enriched peaks and the 6 apo-HpFur exclusive peaks, only 2 were associated with promoters (Figure 3A, lower panel), specifically those of the apo-HpFur repressed *pfr-serB-futB* operon and of the apo-HpFur activated *rs03705-rs03700* operon.

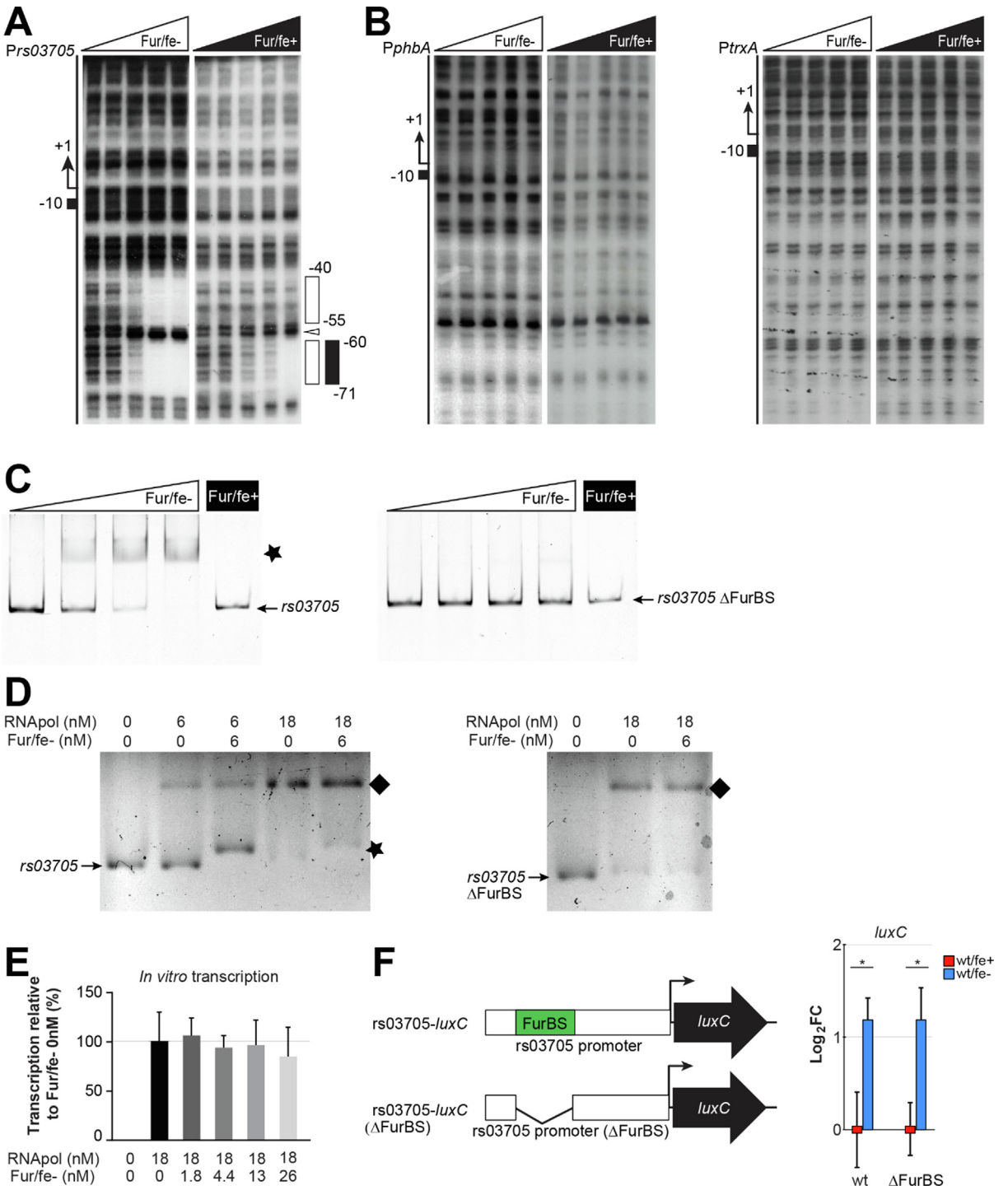

This observation, together with a low enrichment of ChIP reads in correspondence of the apo-HpFur peaks (only 5–10% of the wt/fe− reads mapped on apo-peaks compared to the over 30% obtained in holo-peaks), the absence of known apo-HpFur directly repressed targets, and the very limited correspondence between the apo-HpFur "promoter" peaks and the apo-HpFur activated and repressed TUs determined in the RNA-seq experiment, led us to reconsider the efficiency of wt/fe− immunoprecipitation.

As the apo-HpFur ChIP-seq analysis was scarcely informative, genome-wide identification of the regions bound by HpFur in iron-limiting conditions, hence the determination of apo-HpFur activated and apo-HpFur repressed direct regulons, was not feasible. However, we employed the results of the RNA-seq to guide an extended but not exhaustive determination of the two apo-HpFur direct regulons.

Regarding the apo-HpFur directly repressed regulon, 4 of 32 regulated TUs were already known members: *pfr-serB-futB*, *hydABCDE*, *oorDABC-res-mod*, and *cytc553*.[27,31,34] Hence, we selected the *ccsA*, *homC*, *mdaB*, and *hemN2* TUs to evaluate by DNase I footprinting assay the ability of the HpFur protein to bind to their promoter in fe− and fe+ conditions. For all tested promoters, one or more areas of protection from digestion appeared in the fe− condition when 3–11 nM HpFur dimer was added, indicating a high-affinity interaction between the transcriptional regulator and the DNA (Figure 3B and Figure S3A). All the DNA regions bound by HpFur overlapped the core promoters of the TUs, a position typically associated with repression of transcription. In the fe+ condition, HpFur was unable to interact with the probes, with the exception of the *mdaB* promoter, in which a small area of protection by holo-HpFur appeared from position + 35 to + 49 with respect to the TSS. The DNA probe encompassing the *hydA* promoter was included in the analysis to better characterize the DNA regions bound by apo-HpFur (Figure S3A).

All the DNA sequences protected by apo-HpFur in the DNase I footprinting assays as determined in this work or from literature,[27] and that resulted apo-HpFur repressed were aligned (Figure 3C) to generate the consensus sequence for apo-HpFur direct repression (Figure 3D). Next, we screened the DNA sequences of the promoters associated to apo-HpFur repression (Supplementary Table 3, orange) for the consensus sequence of apo-HpFur repression, excluding those already validated in this study or reported in the literature, the TUs that contained non-iron responsive genes at the 5′-end of the transcript, and those in which no clear indication of the TSS was available. Of the 12 selected TUs, 7 clearly contained the consensus sequence within their core promoters (Figure 3E). The promoters of 4 of these TUs were selected for validation by electromobility shift assay (EMSA) of the binding by apo-HpFur, and a probe on the 16S transcript was employed as negative control (Figure 3F and Figure S3B). Apo-HpFur bound to all the selected promoters at high affinity, as 2.1 nM of the apo-HpFur dimer was sufficient to form a detectable band of protein-DNA complex. The specificity of the complex was confirmed by the absence of detectable DNA-protein complexes with the 16S probe and holo-HpFur.

Analysis of the apo-HpFur directly activated regulon

Of the 26 apo-HpFur transcriptionally activated TUs, only the *rs03705-rny* bicistronic operon

Figure 4. Characterization of HpFur binding and transcriptional regulation at apo-HpFur activated promoters. (A) Validation by DNase I footprinting assay of the direct binding of HpFur on the apo-HpFur activated *rs03705* (HP0761 in strain 26695) promoter. Experimental conditions, numbers, and symbols as in Figure 2. (B) Analysis of direct binding of HpFur on other apo-HpFur activated promoters by DNase I footprinting assay. Radiolabeled probes encompassing *phbA/fadA* (HP0690) and *trxA* (HP0824) promoters were employed for the assay; experimental conditions, numbers, and symbols as in Figure 2. No regions of protection by holo- and apo-HpFur were detected. (C) Validation of the apo-HpFur binding site within the to the *rs03705* promoter by EMSA assay. The DNA probe encompassing the *rs03705* promoter and a mutated variant carrying the deletion of the apo-HpFur binding site (ΔFurBS) as mapped in panel A were employed in the assay. Experimental conditions, numbers, and symbols as in Figure 3. (D) Binding of RNApol on the *rs03705* promoter (wt and ΔFurBS) and competitive/cooperative interference by apo-HpFur. The two DNA probes were incubated with different amounts of *E. coli* RNApol (0, 6, or 18 nM) in presence or not with semi-saturating amounts of apo-HpFur (0, 6 nM of the apo-HpFur dimer). Samples were resolved on a 2% agarose gel; free DNA probes (arrow), RNApo-DNA complexes (diamond), and complexes between apo-HpFur and DNA (star) were visible. (E) In vitro transcription from *rs03705* promoter by RNApol. The chimeric P*rs03705-luxC* DNA probe was incubated with *E. coli* RNApol (0 or 18 nM) in presence of increasing concentrations of apo-HpFur dimers (0, 1.8, 4.4, 13, 26 nM). Transcription levels of the luxC reporter were measured by qRT-PCR. (F) *In vivo* analysis of the role of FurBS *cis* DNA element in the regulation of *rs03705* promoter by apo-HpFur. *H. pylori* mutants carrying the chimeric P*rs03705-luxC* reporter or its ΔFurBS-derivative were treated with iron excesses (fe+) or iron chelator (fe−), and *luxC* transcript levels were determined by qRT-PCR. Statistical analysis as in Figure 1.

resulted associated to an apo-HpFur "promoter" peak (Supplementary Table 6). The direct binding of apo-HpFur on the P*rs03705* promoter was validated by DNase I footprinting assay and the binding site of the HpFur in the fe− condition spanned from position of −40 to −71 from the TSS (Figure 4A). This position is typical of a transcription regulator that promotes transcription, as it localizes the regulator near the αCTD of the RNApol. The ability apo-HpFur to bind the promoter regions of 4 other apo-HpFur activated TUs was checked by DNAse I footprinting assay. Surprisingly, in the selected range of protein concentrations, HpFur could not protect any of the tested probes from DNase I digestion in both fe+ and fe− conditions (Figure 4B and Figure S3C). Thus, HpFur regulation of the expression of these TUs in response to iron is probably indirect.

The *rs03705-rny* promoter appeared to be the only example in our work of direct activation of

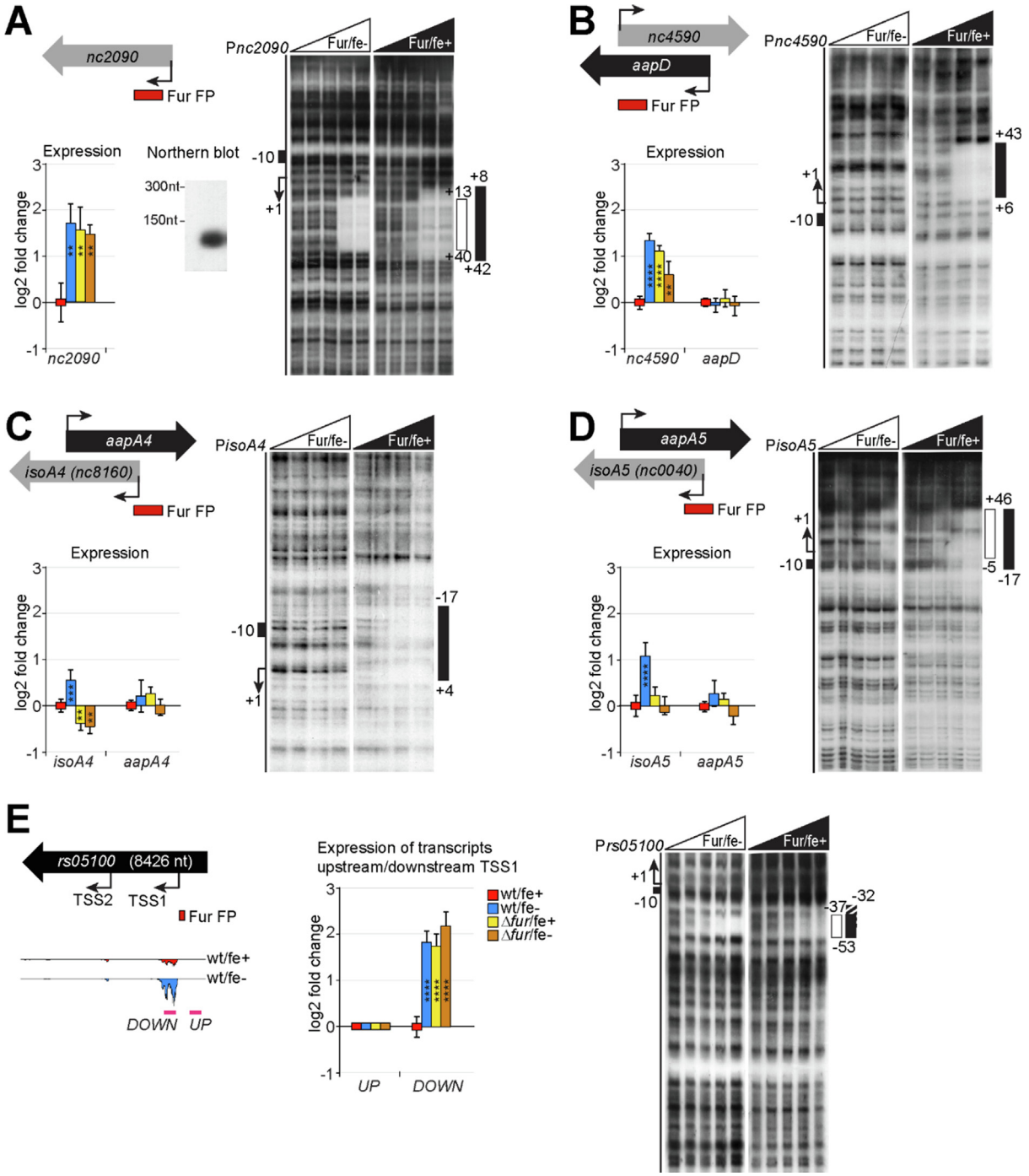

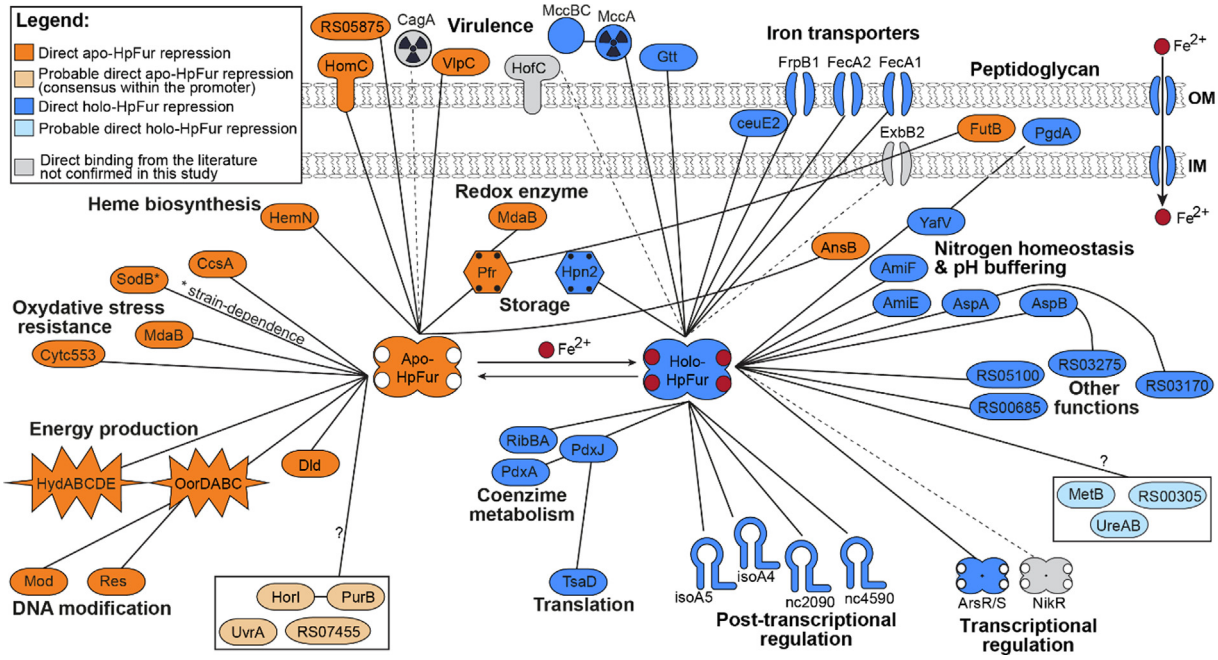

Figure 6. (Re)-definition of the HpFur direct regulons. The network connects holo-HpFur and apo-HpFur to the first gene of TU under their direct transcriptional control. Genes that are part of the same TU are linked to the first gene of their TU. Filled lines/colored proteins indicate new targets validated in this study or those already validated in previous analyses and confirmed here. Holo-HpFur repression and mixed holo-HpFur repression & apo-HpFur induction classes of regulation in blue, apo-HpFur repression in orange. Dashed lines indicate genes (in grey) previously reported as belonging to the holo-HpFur or apo-HpFur direct regulons and not confirmed in this work. Other putative members of the apo-HpFur repressed direct regulon, based on the finding of the apo-HpFur repression consensus sequence in their core promoters, are reported in light orange. Probable other members of the holo-HpFur repressed direct regulon, based on the finding of the holo-HpFur signal in ChIP-seq data, are reported in light blue. Symbols are related to the predicted biological function of the encoded protein.

transcription by HpFur and we sought to better characterize this regulation. Through an EMSA assay, we confirmed that HpFur binds to the *rs03705* promoter only under fe− conditions (Figure 4C, left panel). We repeated the EMSA assay with a mutant of the *rs03705* promoter (*rs03705*ΔFurBS), which was deleted of the apo-HpFur binding sequence identified in the DNase I footprinting assay. Under these conditions, the assay was negative (Figure 4C, right panel), indicating that the deleted sequence is critical for apo-HpFur binding and that the interaction seen in

Figure 5. Analysis of sRNAs and internal transcripts regulated by HpFur in response to iron. (A) Analysis of the non-coding sRNA nc2090. The upper left panel outlines the genomic locus of *nc2090*, and the northern blot assay confirmed the transcript length previously reported.[48] Expression levels were determined by qRT-PCR and reported as described in Figure 1. Direct binding of HpFur on the promoter of *nc2090* was confirmed by DNase I footprinting assay (right panel), with experimental conditions, numbers, and symbols as in Figure 2. (B) Analysis of the *nc4590-aapD* locus in which *nc4590* transcript is partially antisense to *aapD*, as outlined in the upper left panel. Expression levels of *nc4590* and *aapD* were determined by qRT-PCR on cDNAs obtained using target-specific oligos (nc4590pe1 and aapDpe1, respectively). Validation of direct binding of holo-HpFur on the P*nc4590* promoter by DNase I footprinting assay. Experimental conditions, numbers, and symbols as in Figures 1 and 2. (C) Analysis of *isoA4* (*nc8170*) transcript partially antisense to *aapA4* transcript. Same analyses as in panel B. Expression levels of both transcripts were determined by qRT-PCR on cDNAs obtained employing random primers. (D) Analysis of *isoA5* (*nc0040*) transcript partially antisense to *aapA5* transcript. Same analyses as in panel B. (E) Analysis of the *rs05100* gene. The upper left panel outlines the *rs05100* genomic locus along with the position of the HpFur binding site mapped by footprinting assay, RNA-seq traces of wt/fe+ and wt/fe− conditions, and the positions of qRT-PCR amplicons. The middle panel reports the expression levels upstream and downstream TSS1 in the different genotypes and conditions. The right panel reports the DNase I footprinting assay. (A-E) Statistical analyses were performed as described in Figure 1.

the DNase I footprinting assay was not an artifact of the assay. Then we evaluated the ability of apo-HpFur to positively or negatively interfere with the binding of RNApol to the *rs03705* promoter (wt or mutant) in a competitive EMSA assay with the two purified proteins. Each of the two proteins was able to bind the *rs03705* wt promoter, but such binding was neither competitive nor cooperative, as apo-Fur neither reduced nor increased the affinity of RNApol to DNA, respectively (Figure 4D, left panel). As expected, the *rs03705* mutated promoter was bound by the RNApol only (Figure 4D, right panel). Then, an in vitro transcription assay was performed using the chimeric P*rs03705-luxC* construct and the RNApol holoenzyme, in the presence of increasing amounts of apo-HpFur. Coherently with the results of the EMSA assay, apo-HpFur had no effect on the RNApol transcription efficiency from the *rs03705* promoter (Figure 4E).

As none of the in vitro assays showed a possible positive interaction between apo-HpFur and RNApol on the *rs03705* promoter to support the apo-HpFur direct activation of transcription, we studied the regulation of *rs03705* promoter in vivo. The chimeric P*rs03705-luxC* and the *rs03705*ΔFurBS-*luxC* mutant were inserted into the bacterial genome, and the iron-dependent transcriptional response of the TU was studied. Both constructs showed increased transcript levels in the fe− condition (Figure 4F), indicating that the HpFur binding site determined by in vitro and in vivo assays is not critical for mediating HpFur-dependent regulation in vivo.

Analysis of unannotated sRNAs and transcripts from internal TSS regulated by HpFur in response to iron

Manual inspection of both ChIP- and RNA-seq traces showed additional unannotated *H. pylori* transcripts, that appear to be directly regulated by HpFur in response to iron levels. Given the increasing interest in non-coding RNAs roles we cross-mapped on G27 those identified by Sharma et al in strain 26695.[48] The RNA-seq traces showed that *nc2090* sRNA[48] was expressed at lower levels in the wt/fe+ condition with respect to the wt/fe−, whereas in the Δ*fur* strain the transcript resulted de-repressed. Thus, *nc2090* is repressed by holo-HpFur. In the holo-HpFur ChIP-seq data, the promoter upstream of the transcript showed a small peak in the wt/fe+ condition compared to the background. Northern blot analysis confirmed the expression of a small transcript of about 80 nucleotides long, and its regulation was validated by qRT-PCR (Figure 5A). Direct binding of HpFur to the P*nc2090* promoter in fe+ (5.6 nM of the holo-HpFur tetramer) and fe− (34 nM of the apo-HpFur dimer) conditions was determined by DNase I footprinting analysis. Accordingly, the holo-HpFur operator overlaps the core promoter of P*nc2090*, suggesting that holo-HpFur directly represses the sRNA.

Manual inspection of the RNA-seq traces allowed the identification of the *nc4590*, *isoA4* (*nc8170*), and *isoA5* (*nc0040*) sRNAs that showed reduced levels in wt/fe+ condition with respect to wt/fe−. These transcripts were reported to be antisense to the *aapD*, *aapA4*, and *aapA5* transcripts,[48] respectively. In RNA-seq data and subsequent validations by qRT-PCR, *nc4590* was repressed in the wt/fe+ condition and de-repressed in the fe− condition and Δ*fur* genotype, indicating a holo-HpFur repression, while the transcript from the other DNA strand resulted not regulated in the conditions tested. Inspection of ChIP-seq data of holo-HpFur showed a small peak. Accordingly, DNase I footprinting allowed validation of a holo-HpFur binding site on the *nc4590* promoter (Figure 5B). In contrast, *isoA3* and *isoA5* resulted more expressed in wt/fe− than in wt/fe+, Δ*fur*/fe+, and Δ*fur*/fe− conditions (RNA-seq and qRT-PCR; Figures 5C and 5D), indicating a transcriptional activation by apo-HpFur. Transcripts from the other DNA strand showed no regulation in the conditions/genotypes tested. Direct binding of HpFur on the *isoA4*, and *isoA5* promoters was validated by DNase I footprinting analysis. Surprisingly, high-affinity areas of protection overlapping the core promoters of the two transcripts were observed in the fe+ condition (5.6–17 nM of the holo-HpFur tetramer), while in the fe− condition the protection was absent in P*isoA5* and with reduced affinity (112 nM) and extension for P*isoA5*.

Finally, the manual revision of the −omic traces allowed the re-definition of the *rs05100* genomic locus. Specifically, RNA-seq traces showed that the long *rs05100* gene (8426 nt) is not associated with a transcript that covers the entire CDS, but the first part of the locus is not transcribed at all, while in the middle of the CDS two transcripts are detectable, one of which is repressed by holo-HpFur in response to iron. The direct binding of holo-HpFur on the promoter of this transcript was confirmed by DNase I footprinting assay.

Discussion

The Fur protein is the master regulator of iron homeostasis in prokaryotes and functions mainly by repressing transcription of target genes with iron used as a co-repressor (holo-HpFur repression). In addition to this regulatory mechanism, the HpFur protein of *H. pylori* and of some other bacteria is also able to repress the transcription of a different subset of genes when iron levels are low (apo-HpFur repression).[24–26] In this case, iron acts as an inducer of transcription because the transcriptional promoter repression is released when intracellular iron level increases. Thus, these forms of HpFur protein are transcriptional commutators, with apo- and holo-HpFur functioning as two transcriptional repressors, each with

a distinct mechanism of operation, specific targets, and imposing transcription repression which is dictated to opposite conditions of iron levels. *H. pylori* is highly sensitive to adequate levels of iron ion, since many iron-dependent proteins are absolutely necessary for the bacterium survival in the gastric niche and the colonization of this hostile environment, whereas iron overload is highly detrimental. Moreover, HpFur plays a central role in cell regulation, as it is the master regulator of other pivotal circuits of adaptation to environmental variations, such as acclimation to acidic pH, chemotaxis, oxidative stress response, and nickel homeostasis.[49] Thus, it is not surprising that HpFur null mutants are defective in host colonization.[4]

Given the importance of HpFur in cell regulation, both apo- and holo-HpFur regulons have been extensively investigated in single-target and genome-wide studies, although -omic approaches have not been able to distinguish between direct and indirect regulons or to relate the binding of HpFur on the genome to regulation. In this context, the strategy of integrating two powerful -omic approaches that simultaneously detect transcription responses to iron and the in vivo binding of HpFur to DNA allowed genome-wide identification of holo-HpFur direct regulon and a strategy to expand the apo-HpFur direct regulon, at least for the experimental conditions tested (Figure 6). To our knowledge, this is the first ChIP sequencing analysis of HpFur.

Prevalent binding of holo-HpFur in intracistronic regions. ChIP-seq analysis of holo-HpFur showed that, in vivo, most of the binding sites of HpFur are located within coding sequences (80%). Interestingly, most of these CDS are not regulated in response to iron levels, and the rare exceptions almost invariably contain additional HpFur binding sites on their promoters that are exploited by HpFur to exert iron-dependent regulation. Intracistronic binding sites could be related to internal cryptic promoters for transcription from alternative TSS or for expression of antisense regulatory RNAs. However, RNA-seq analysis did not detect any asRNA downstream of these loci, nor did it show differences in transcript levels between the regions upstream and downstream of the binding sites in any condition/genotype tested. The latter observation was further confirmed for *amiA* by qRT-PCR (Figure 2G). Intracistronic binding unrelated to transcriptional regulation is not uncommon in prokaryotes, including *H. pylori*,[50,51] and Fur of other bacteria showed medium to high proportions of intracistronic binding sites (37% in *Pseudomonas syringae*,[52] 41% in *Bacillus subtilis*,[53] and 73% in *Mycobacterium avium*.[54] These non-regulatory loci likely depend on the intrinsic affinity of the transcriptional regulators to DNA[55] and may constitute parking bays of unused Fur protein or a way to increase the amount of the protein in the immediate vicinity of regulatory sites. Furthermore, as holo-HpFur is able to form high-order protein complexes and knot the DNA it binds,[39] these loci could be involved in the regulation of distant sites through DNA compaction, or they could be evidence of nucleoid-like properties of HpFur for chromosome organization. The latter hypothesis will be the subject of a dedicated article.

The high density of holo-HpFur binding sites in the genome observed here and in,[28] and the heavy prevalence of intracistronic sites have 3 important consequences: (i) the binding sites that overlap with promoters are overwhelmed by intracistronic peaks, leading to suboptimal identification of the formers. Accordingly, manual inspection of the ChIP-seq data allowed the identification of important holo-HpFur promoter peaks that were missing in the analysis. (ii) Although intracistronic peaks are not locally related to transcription regulation, these HpFur binding sites may modulate chromosome organization and compaction, eventually affecting transcription. Hence, the transcript levels of some genes may be influenced by the presence/absence of HpFur *per se*, with effects on the wt and Δ*fur* comparisons. For example, *amiE*, *aspA*, and *amiF* were classified as mixed holo-HpFur repressed & apo-HpFur activated TUs and in our analysis we validated the holo-HpFur direct repression but the apo-HpFur direct activation was not confirmed. The lower transcript levels of these genes in the Δ*fur* genotype with respect to the wt/fe− condition that led to the classification of apo-HpFur activated TUs, may be alternatively explained as positive effects of HpFur *per se* on the transcription of these genes, and the absence of the transcriptional regulator in the Δ*fur* mutant may result in reduced expression of these loci. (iii) Determination by footprinting assay of the exact DNA sequences bound by HpFur and analysis of the distance of the binding sites from the TSS, the affinity of protein-DNA interactions, the extension of the protection, and the changes in fe+ and fe− conditions, are all helpful information to determine the class of HpFur regulation correctly. Going back to the example above, *amiE*, *aspA*, and *amiF* show a clear protection by holo-HpFur, while in fe− condition, the protection is absent (*amiE*), or is present at lower affinity, with a reduced extension (*aspA*), and invariantly positioned on the core promoter, a position poorly compatible with transcriptional activation (Figure 2D and Figure S2C). These observations sustain holo-HpFur direct repression of these promoters, but not the apo-HpFur activation.

Holo-HpFur directly repressed regulon. Most of the genes known to be directly repressed by HpFur in fe+ condition (in both holo-HpFur repression and mixed holo-HpFur repression & apo-HpFur activation) were confirmed, including iron importers (*frpB1*, *fecA1*, *fecA2*), enzymes for the biosynthesis of vitamin B2 and B6 (*pdxA*, *pdxJ*), virulence factors (*ggt*), the nickel storage

protein *hpn2*, the transcriptional regulator *arsR* that regulates responses to acid, and *fur* itself. In addition, 8 new operons were shown to be part of the holo-HpFur directly repressed regulon.

The *ribBA* gene, which is involved in both riboflavin synthesis and iron uptake, is contained in a monocistronic operon and was already identified as a putative gene of the holo-HpFur directly repressed regulon. However, the class of regulation was uncertain (holo-HpFur repressed in[45,43,56,57]) or holo-HpFur activated in,[29] and its genomic region was reported to be bound in vivo by HpFur in fe+ condition.[28] Our analysis showed that *ribBA* is directly repressed by holo-HpFur (Supplementary Table 4), and the holo-HpFur binding site was mapped on the core promoter of the operon (Figure S2B), a typical position for transcriptional repression. The link between riboflavin synthesis and iron uptake has not been fully explained. Nevertheless, it has been proposed that the enzymatic activity of RibBA protein or riboflavin itself increases the reduction of Fe (III) to Fe (II), which is more soluble and easier to adsorb. In addition, RibBA protein or its metabolites have been shown to possess hemolytic activity to increase the bioavailability of iron ions through the destruction of iron-rich erythrocytes.[57,58] Holo-HpFur repression of *ribBA* is consistent with these activities of the protein.

amiF is another gene whose regulation by HpFur has long been debated since there are studies that have proposed its HpFur-mediated repression in iron-rich conditions[45] and direct binding of holo-HpFur to the promoter of this monocistronic operon,[28] while other findings have excluded this gene from direct and indirect HpFur regulons.[42] In our analysis, the *amiF* core promoter resulted directly repressed by the holo-HpFur. The formamidase activity of AmiF is related to nitrogen metabolism and pH buffering and, together with the cognate AmiE, which has similar functions and is also repressed by holo-HpFur, are involved in HpFur-dependent acid response and perhaps also in iron homeostasis through modification of the environmental pH.[42] Discrepancies from previous data[42] may be attributed to the experimental conditions or the bacterial strain employed.

Another gene we found part of the holo-HpFur directly repressed regulon is *yafV*. The encoded protein is annotated as 2-oxoglutaramate amidase and catalyzes the breakdown of the substrate and ammonia production.

Holo-HpFur directly represses the *mccB-mccC* operon (Figure 2B), which expresses factors for Microcin C (McC) biosynthesis.[59] McC and McC-like compounds are post-translationally modified small peptides secreted by some bacterial species into the surrounding medium and exert antibiotic effects on other bacteria sharing the same ecological niche. The biosynthesis of microcins involves at least MccA, MccB, and MccC, and additional factors can be involved.[59] Many *H. pylori* strains harbor plasmids containing the homologs of *mccB* and *mccC*, while the short peptide homolog of *E. coli mccA* was missing. However, a small ORF of 7 amino acids maps in the 5′ region of the *mccB-mccC* transcript; a Shine Dalgarno sequence precedes it and has been proposed to be the *mccA* gene in this bacterium – although the amino acidic sequence diverges from that of other known microcins –, and this polypeptide is processed in vitro by the purified MccB protein.[59] Hence, a complete system for extracellular McC production is likely present in these plasmid-positive strains and, although still poorly characterized, could be a bactericidal factor against co-commensal bacteria. Holo-HpFur repression of the microcin operon is probably a mechanism for modulating the toxic arsenal of the bacterium in response to the need to acquire iron from the environment. When iron is abundant, holo-HpFur represses the expression of the *mccA-mccB-mccC* operon, reducing the amount of microcin and, consequently, the production of bactericidal compound; conversely, in iron-starved conditions, the repression of the operon is relieved, increasing the production of microcin. Competition studies with commensal bacteria and microcin-negative *H. pylori* strains will be needed to evaluate this effect.

Another gene directly repressed by holo-HpFur is *rs00685*. This gene codes for a very small and still uncharacterized protein (45aa long), which is predicted to be a membrane lipoprotein and has been observed in the protein fraction of OMVs. Although its function remains unknown, its localization suggests it may be involved in host interaction and pathogenesis.

Our analysis, in addition, pinpointed *nc2090* as the first small non-coding RNA directly repressed by holo-HpFur. In a previous transcriptional analysis performed in strain 26695,[48] *nc2090* was proposed as part of the type VIII toxin-antitoxin system, in which a non-coding RNA (the antitoxin) is partially antisense to a transcript that codes for a toxin against other bacteria.[60] Typically, the toxin is tightly controlled so that when there is no need to compete for the environmental niche, the antitoxin is expressed at high levels and, in turn, inhibits transcription and/or translation of the toxin. Conversely, when the bacterium needs to attack other bacteria, it downregulates the antitoxin transcript levels and allows toxin expression. In strain 26695, it has been reported that *nc2090* is antisense to the uncharacterized putative toxin AapC1 and this genomic region is duplicated in the *nc5320-aapC2* locus (100% identity). In strain G27, *nc2090-aapC1* is highly conserved (Figure S4C), while *nc5320-aapC2* is defective and highly mutated with respect to the *nc2090*-AapC1 locus (Figure S4D). Transcriptional analysis in strain G27 validated the expression and the regulation of *nc2090* with multiple techniques (Figure 5A),

but *aapC1* transcript was almost undetectable in RNA-seq, and all attempts to validate this RNA failed. As a previous study on strain 26695[48] did not report the *aapC1*/*aapC2* TSSs, there is no validation of these transcripts, and genomic inspection shows a Shine-Dalgarno sequence rather far upstream from the start codon (Figure S24C). Therefore, we consider *nc2090* a holo-HpFur-repressed ncRNA. Although the regulation of *nc2090* parallels other virulence factors, its potential role in HpFur-dependent post-transcriptional regulation is still to be determined. It is worth noticing that G27 *nc5320* has a promoter region almost identical to that of *nc2090*, but the holo-HpFur binding site, located at position +8 to +42 relative to the TSS, is much lesser conserved. Accordingly, *nc5320* in strain G27 is expressed but does not respond to iron levels nor is bound by HpFur. This is further evidence for specific holo-HpFur direct repression of *nc2090*.

Another type VIII toxin-antitoxin directly regulated by holo-HpFur is *nc4590-aapD*, in which, unlike the locus just described, both transcripts were detected by RNA-seq and qRT-PCR (Figure 5B). Holo-HpFur binds to the promoter of *nc4590*, directly repressing its transcription when iron is abundant. Accordingly, its levels in Δ*fur* mutant are de-repressed regardless of iron levels, confirming its direct repression by holo-HpFur. The *aapD* transcript, which encodes for the predicted toxin, did not appear to be regulated by HpFur, nor did it respond to iron levels variation. Regulation of *aapD* by *nc4590* likely occurs post-transcriptionally.

The *rs05100* gene was a new hit of the holo-HpFur directly repressed regulon, although the only binding site of the HpFur was located within the CDS. Analysis of the locus showed that a mRNA encompassing the entire annotated CDS was missing, and small transcripts were detectable in specific parts of the operon. One of these short transcripts appeared repressed by holo-HpFur and, accordingly, the intracistronic holo-HpFur binding site mapped on the core promoter of this transcript. Analysis of the smaller transcript identified a new CDS with homology to helicases.

Further inspection of the -omics data allowed for the inclusion of other genes in the holo-HpFur repression or mixed holo-HpFur repression & apo-HpFur activation. Specifically, *amiE* was shown to be directly repressed by holo-HpFur, confirming previous observations.[33,45,29,42] In addition, the aspartate ammonia-lyase *aspA* and the aspartate aminotransferase *aspB* genes were shown to be directly bound and repressed by holo-HpFur. Both encoded proteins are involved in aspartate deamination, with direct implications in nitrogen homeostasis, degradation of host metabolites, and, at least for AspA, in ammonia production and pH buffering. Similarly to *ggt*, holo-HpFur direct repression of *amiE* and *amiF* is related to the acid environment response and the degradation of host metabolites.[61] A very weak signal of holo-HpFur in the ChIP-seq data on the promoter of *ceuE2* confirmed the previous observations.[40] Manual inspection of the ChIP-seq data of the TU promoters in Supplementary Table 4 suggested that *metB* and *rs00305*, which had already been reported as repressed by holo-HpFur[33,45,29] are most likely part of the holo-HpFur directly repressed regulon. Another candidate is the *ureA-ureB* which was associated with a strong holo-HpFur peak that, although validated (Figure S5), is positioned far upstream of the TSS (>150nts), a less frequent position for direct transcriptional repression. As the P*ureA* promoter is directly regulated by other transcriptional regulators (NikR and ArsR),[38,50] the regulatory mechanisms controlling this promoter could be very complex and deserve dedicated studies. The consensus sequence for holo-HpFur repression was determined (Figure 2F) and showed a classical 7-1-7 dyad typical of the Fur boxes.[8,27,29]

Holo-HpFur directly activated regulon. Of the 5 TUs of the transcriptionally activated by holo-HpFur (Supplementary Table 3), none showed a holo-HpFur peak proximal to the promoter (bioinformatic analysis and manual inspection). Therefore, holo-HpFur directly activated regulon is likely absent in *H. pylori* in the experimental conditions tested.

Apo-HpFur directly repressed regulon. *pfr-serB-futB* (ferritin, phosphoserine phosphatase fucosyltransferase), *cytc553* (cytochrome *c*), *hydABCDE* (hydrogenase), and *oorDABC* (2-oxoglutarate oxidoreductase) operons were already validated members of the apo-HpFur directly repressed regulon.[23,27,28,33,45,32,34,31,62] As expected, under conditions of iron starvation, *H. pylori* exploits apo-HpFur to directly repress the expression of iron storage proteins (ferritin) and iron-consuming enzymes (cytochrome *c*, hydrogenase, and 2-oxoglutarate oxidoreductase employ iron as co-factor.[63–65] FutB is involved in the synthesis of the Lewis X trisaccharide, the major component of lipopolysaccharides. Thus FutB is involved in virulence and immune-escape mechanisms,[66] and SerB is involved in serine biosynthesis. Repression by apo-HpFur of these two enzymes could be related to the modulation of virulence and metabolism in iron starvation conditions. Our validation by footprinting assay included P*cytc553* and P*hydA* to increase the resolution of the apo-HpFur binding sites within these promoters.[34] For the latter, the previously reported apo-HpFur binding site mapped far upstream of the TSS (from position −84 to −156), a less frequent position for direct transcriptional repression.[34] In our hands, apo-HpFur bound to the core promoter of *hydA* (Figure 3A). This apparent discrepancy is resolved in the following sections. Although the ChIP-seq data of apo-HpFur were not good enough to be integrated with the RNA-seq data, we partially extended the

apo-HpFur directly repressed regulon by validating a subset of genes identified in the transcriptional analysis.

The *hemN* gene is divergently oriented from *cytc533*, their core promoters partially overlap, and the binding site of apo-HpFur falls within this region (Figure 4C). Therefore, it is not surprising that these genes are directly co-repressed by apo-HpFur. The *hemN* gene is annotated as a coproporphyrinogen-III oxidase involved in heme biosynthesis, although this protein family includes enzymes with different functions[67] and is predicted to contain an iron-sulfur cluster.[65]

Similarly, *mdaB* is divergent from the *hydABCDE* operon, and both transcripts were confirmed to be directly repressed by apo-HpFur. The two divergent promoters have their core sequences more than 100 nt apart, and apo-HpFur has two binding sites, one for each core promoter. Notably, the region previously reported to be bound by apo-HpFur on P*hydA*[34] corresponds to the binding site of HpFur on the core of P*mdaB*. The MdaB protein is annotated as an NADPH quinone reductase, involved in protection from oxidative stress and important for host colonization.[68] Since iron is a major source of ROS and oxidative stresses, expression of this enzyme is repressed by HpFur in iron-limiting conditions, that is, when the bacterium is likely exposed to lower levels of oxidant species.

Another new entry for the apo-HpFur directly repressed regulon is *ccsA*, annotated as either a transmembrane cytochrome *C* biogenesis protein or a secreted cytochrome c551 peroxidase. Sequence analysis attributed the protein to the cytochrome c551 peroxidase family because they have a more similar tertiary structure, a signal peptide for periplasmic secretion is predicted at the N-terminus of the protein, and there are no predicted transmembrane domains. CcsA contains 2 conserved CXXCH motifs for binding a pair of hemes, which the bacterium uses to catalyze the reduction of peroxides.[69] Since CcsA is an iron-consuming protein, its repression in fe− is probably a way to reduce iron utilization in iron-limiting conditions.

The *homC* gene codes for a proteolytic-sensitive outer membrane protein involved in adhesion and adaptive antigenic variation.[70] Its inclusion in the apo-HpFur directly repressed regulon indicates that the bacterium modulates virulence and adhesion in response to iron levels.

Sequence alignment of the regions protected in the footprints assays allowed us to refine the previous consensus sequence of for apo-HpFur direct repression.[27,34] This consensus sequence was found within the core promoters of additional 7 TUs of the apo-HpFur directly repressed regulon, and all 4 tested promoters were confirmed to be part of the apo-HpFur directly repressed regulon. These include the *vlpC* gene that codes for a VacA-like toxin involved in host colonization[71] but that recently has been reported to be the locus of a not yet characterized CRISPR-like system of *H. pylori*; the *rs05875* gene that codes for a protein involved in the efflux of antibiotics and detoxification[72]; and AnsB which is important for host colonization for its ability to buffer the low pH of the stomach and deplete gastric and immune cell defenses.[73]

It is worth noting that genes repressed by apo-HpFur include enzymes involved in protection from oxidative stress. Because ROS mostly originate from metal-catalyzed reactions (especially iron ions) and from host defenses, repression of this regulon limits iron consumption when the level of iron ions is low enough to be harmless to the cell. However, in this condition the bacterium would be more susceptible to the host immune system that attacks the pathogen with oxidant species. Intriguingly, when *H. pylori* is exposed to both iron-starvation and oxidants, HpFur specifically derepresses the apo-HpFur directly repressed regulon[46] to restore the expression of oxidant-protective proteins and reactivate its defenses.

Apo-HpFur directly activated regulon. Although HpFur has traditionally been considered a transcriptional repressor for both non-metaled and iron co-factored forms of the TR, global transcriptional analysis classified some TUs and *isoA4* and *isoA5* ncRNAs into the apo-HpFur activated and mixed holo-HpFur repressed & apo-HpFur activated classes of regulation (Figure 5C and 5D). Attempts to discriminate between direct and indirect regulation showed that *isoA4* and *isoA5* ncRNAs belong to the holo-HpFur directly repressed regulon, and the apo-HpFur transcriptional activation of these transcripts is likely apparent. Specifically, both promoters are bound by holo-HpFur on regions of DNA overlapping the core promoters, a typical position for transcription repression, and both transcripts showed reduced levels in the wt/fe+ condition compared with wt/fe−. The reduced levels in Δ*fur* strain may be due to the positive effects of HpFur on transcription (see previous paragraph in the discussion). Although *isoA4* and *isoA5* are transcribed antisense to the *aapA4* and *aapA5* putative toxins and it was proposed that they control the expression of the toxins,[48] the actual production of the toxic peptides has not been shown, and the holo-Fur directly repressed *isoA4* and *isoA5* transcripts might function as ncRNAs.

Of the other promoters analyzed, 4 out of 5 resulted not directly bound by HpFur (apo or holo), indicating that regulation on these targets is indirect. The only exception is the *rs03705-rny* bicistronic operon in which apo-HpFur binds to a DNA region upstream of the core promoter. In contrast to transcription repression in which the steric hindrance of the core promoter by the transcriptional regulator is frequently sufficient to

repress the promoter, positive regulation of transcription often requires cooperative interactions with RNApol. A deeper characterization of this locus and of apo-HpFur and RNApol interplay failed to show any direct transcriptional activation by apo-HpFur, suggesting indirect regulation by HpFur. Hence, no TU was associated to the apo-Fur directly activated regulon.

In conclusion, the double-omic approach allowed the (re)-definition of apo-HpFur and holo-HpFur direct regulons, confirming that, although the classes of HpFur regulation are 5, only the two in which HpFur functions as a repressor are associated with direct regulons. In addition to genes involved iron homeostasis, the holo-HpFur directly repressed regulon contains genes for ammonia production – likely associated with pH buffering –, virulence factors, transcriptional and post-transcriptional regulators, indicating low-aggressive phenotype, and low ammonia production when iron is abundant. Conversely, apo-HpFur directly repressed regulon contains, in addition to genes involved in iron homeostasis, genes for redox defense and energy production, and several factors involved in virulence, host colonization, and defense. In iron-starved conditions, repression of these factors and de-repression of the holo-HpFur repressed regulon suggest increased iron uptake and reduced consumption of the metal, but also a metabolic shift, increased virulence and ammonia production, and activation of transcriptional and post-transcriptional regulatory programs.

Materials and Methods

Bacterial strains and growth conditions. All *H. pylori* strains used are listed in Supplementary Table 7. Bacteria were recovered from frozen glycerol stocks and propagated on BBL Brucella agar (BD) plates containing 5% FBS (Euroclone). Bacteria were grown at 37 °C in jars using CampyGen™ (Oxoid) gas–packs or in a water–jacketed thermal incubator (9% CO_2 and 91% air atmosphere, with 95% humidity) for 24–48 hr. Liquid cultures were grown in BBL Brucella Broth (Merck) supplemented with 5% FBS at 37 °C in glass flasks with gentle agitation (125 rpm). For fe– and fe+ treatments, bacterial cultures were exposed to 150 μM 2,2′-Dipyridyl (Merck) and 1 mM $(NH_4)_2Fe(SO_4)_2$ (Merck), respectively, for 20 min. *E. coli* strains were grown in Luria–Bertani (LB) agar or LB broth (BD). When required, 100 μg/ml ampicillin (Merck) or 30 μg/ml chloramphenicol (Merck) was added.

DNA manipulations. DNA amplification, restriction digestions and ligations were carried out with standard molecular techniques, with enzymes purchased from New England Biolabs.

RNA preparation, qRT-PCR assays, primer extension and Northern blot. Bacterial cultures were grown to OD_{600} of 1.0–1.1 and split into 2 sub–cultures of 5 ml each that were treated either with 1 mM $(NH_4)_2Fe(SO_4)_2$ (fe+) or 150 μM 2,2′-Dipyridyl (fe–) for 20 min. Treatments were stopped by the addition of 625 μl RNA stop solution (95% ethanol, 5% acid phenol; Thermo Fisher Scientific) and total RNA was purified using 1 ml of TRIzol (Thermo Fisher Scientific) for each sample, following the manufacturer instructions. RNA samples were treated with RapidOut DNA Removal Kit (Thermo Fisher), reverse-transcribed with Random hexamer (Invitrogen) and RevertAid First Strand cDNA Synthesis Kit (Thermo Fisher), then the qRT-PCR assays were performed as in.[50] Where indicated, 10 pmol of gene-specific primers were employed instead of random primers. Primer extension analysis was performed using 15 μg of total RNA and 0.1 pmol of radiolabeled probe. Northern blot assay was performed using 15 μg of total RNA and 1.25 pmol of radiolabeled oligo probe. See[50] for the details.

RNA-sequencing: library preparation, sequencing and analyses. Ribosomal RNAs were depleted starting from 1 μg of total RNA from each of the conditions analyzed by using the RiboZero Gram negative kit (Epicentre, Illumina), strand specific RNA-seq libraries were prepared by using the ScriptSeq™ v2 RNAseq library preparation kit (Epicentre, Illumina) starting from 50 ng of previously rRNA-depleted RNA from each biological replicate and for all the conditions analyzed. Then each library was sequenced on a MiSeq Illumina sequencer and 76 bp paired end reads were produced obtaining a minimum of 9 million reads per sample. The analysis has been performed as described in detail in,[50] briefly Bowtie 2 (v2.2.6)[74] was used to align raw reads to *H. pylori* G27 genome, obtaining over 96% of mapped reads. A modified version *H. pylori* G27 annotation based on RefSeq GCF_000021165.1[75] BEDTools (v2.20.1)[76] and SAMtools (v0.1.19)[77] were used to verify the library preparation and sequencing performances and to produce strand specific gene level counts as reported in.[78] Ribosomal RNA depletion produced a reduction of ribosomal reads to less than 7% of the total mapping, 99% of the annotated transcripts were covered by at least one strand specific read and a minimum of 60 reads were counted on 90% of them, see Supplementary Table 1. The R package DESeq2 (v1.4.5)[79] was then used to normalize the counts and to identify iron-dependent differentially expressed genes (iDEGs) in the fe+ vs fe– comparison, showing BH (Benjamini-Hochberg) adjusted p-value (padj) lower than 0.01 and log2 fold changes |log2FC| > 1. HpFur-dependent differentially expressed genes in response to iron (fDEGs) were identified as transcripts with |log2FC| > 0.65, padj < 0.01 and a |log2FC(wt) – log2FC(Δ*fur*)| > 0.85. To classify

fDEGs in the 5 HpFur regulatory classes, gene expression was considered different between wt and Δ*fur* genotypes when |log2(wt/Δ*fur*)| > 0.5 in fe+ or fe− conditions. Bam files are publicly available at Sequence Reads Archive (SRA) under accession number BioProject PRJNA313048.

Overexpression and purification of recombinant HpFur protein. Recombinant His_6-HpFur protein was overexpressed and purified under native conditions as previously described.[31] The N-terminal histidine-tag was removed using thrombin protease (10 U/mg; Amersham GE Healthcare), according to the instructions of the manufacturer. The resulting protein preparations were dialyzed overnight against PBS for antibody preparation and purification or against HpFur footprinting buffer (10 mM Tris-Cl pH 7.85, 50 mM NaCl, 10 mM KCl, 0.02% Igepal, 10% glycerol, 0.1 mM DTT; all from Merck) for the DNA-binding experiments. Dialyzing membranes with a cut-off of 3KDa were employed to remove the cut His-tag. A Bradford colorimetric assay (BioRad) was used to quantify the protein fractions with bovine serum albumin as standard.

Preparation of a polyclonal anti-HpFur antibody. The anti-HpFur antisera were generated by immunizing rabbits with affinity-purified recombinant HpFur protein (without His-tag) dissolved in PBS, by Biotem Custom Antibodies and Services. After the final bleed, a portion of the antisera was purified by affinity purification: 9 mg of purified HpFur protein dissolved in 3 ml PBS were mixed with 200 mg of dry NHS-Activated agarose resin (Thermo Scientific) and the chemical coupling of HpFur to the resin was carried out for 16 h (1 h at 25 °C and 15 h at 4 °C). Remaining active sites of the resin were quenched with glycine according to the instructions of the manufacturer, followed by 2 washes with PBS and incubation with the antisera (16 h at 4 °C) for the binding of anti-HpFur antibodies. Resin was washed twice with PBS, then the purified anti-HpFur antibodies were eluted using 0.1 M glycine-HCl (pH 2.5) and subsequently neutralized by the addition of 1 M Tris (pH 9). In parallel, another portion of antisera was chemically purified by 3 sequential precipitations with 35% saturated $(NH_4)_2SO_4$ and subsequent dissolution in water. Both purifications were assayed by western blot (WB) analysis on *H. pylori* total extracts.[50] The partially chemically purified anti-HpFur antibody was serially diluted and assayed in WB analysis; the dilution that showed a signal similar to that produced by the affinity purified antibody was mixed in a 1:1 (volume/volume) proportion for the ChIP-sequencing experiments.

Chromatin Immunoprecipitation with a polyclonal α–HpFur antibody. Bacterial cultures were grown to OD_{600} of 1.0–1.1 and split into 2 sub–cultures of 50 ml each that were treated either with 1 mM $(NH_4)_2Fe(SO_4)_2$ (fe+) or 150 μM 2,2′-Dipyridyl (fe−) for 20 min. Samples were treated as previously described.[50]

ChIP-sequencing: library preparation, sequencing and analysis. Illumina libraries were prepared, for each of the conditions and strains analyzed from 5 ng each of the two biological replicates following the Illumina TruSeq ChIP-seq DNA sample preparation protocol; then each library was sequenced on a MiSeq Illumina sequencer and a minimum of 2 million 51 bp single stranded reads were produced. Bowtie 2 (v2.2.6)[74] was used to align raw reads to *H. pylori* G27 genome (RefSeq GCF_000021165.1) as detailed in,[50] obtaining over 97% of mapped reads (see Supplementary Table 1).The quality of ChIP-Seq data was evaluated following ENCODE quality metrics and the numerical values obtained are provided in Supplementary Table 1. Irreproducible Discovery Rate procedure (IDR v 2.0.2)[80] following ENCODE guidelines and using Homer (v4.7.2)[81] as peak caller, was performed to measure sample reproducibility and to identify consistent peaks as detailed in.[50] The "Fold Change vs Control" column was selected as ranking column for IDR calculations, Δ*fur*-iron pooled samples were used as input/background for all the other experimental conditions. Peaks were manually classified as "promoter peaks" if centered −100/+30 from a TSS, as "intragenic peaks" if centered inside annotated genes and more than 30 nt apart from a TSS, and "intergenic peaks" if centered in unannotated regions and located farther than 100 nt form a TSS. TSS annotation was obtained cross-mapping onto G27 genome the 50 nt sequence upstream the 26,695 published list of TSS[48] and manually verifying the correspondence of the loci.

DNase I footprinting. The DNA probes were prepared as follows: 1 pmol of pGEM-P*ggt*, pGEM-*amiA*, pGEM-*hefA*, pGEM-P*ribBA*, pGEM-P*amiF*, pGEM-P*mccB*, pGEM-P*rs00685*, pGEM-P*amiE*, pGEM-P*aspA*, pGEM-P*aspB*, pGEM-P*hydA*-P*mdaB*, pGEM-P*ccsA*, pGEM-P*homC*, pGEM-P*hemN*-P*cytc553*, pGEM-P*rs03705*, pGEM-P*phbA*, pGEM-P*trxA*, pGEM-P*hopC*, pGEM-P*tsa*, pGEM-P*nc2090*, pGEM-P*nc4590*, pGEM-P*isoA4*, pGEM-P*isoA5*, pGEM-P*rs05100*, pGEM-P*yafV*, and pGEM-P*ureA* vectors were linearized either with NcoI or NdeI, dephosphorylated with calf intestinal phosphatase and labeled at the 5′ ends with 2 pmol of [γ–^{32}P] ATP (6000 Ci/mmol; PerkinElmer) by using T4 polynucleotide kinase. The labeled DNA probe was further digested either with NdeI or NcoI and the products were separated by native polyacrylamide 4% gel electrophoresis, eluted and purified as previously described.[46] pGEM-P*hydA*-P*mdaB* vector was linearized either with NcoI or NdeI and labeled to obtain the probes for P*hydA* and P*mdaB*. The binding reactions were carried out by using approximately 20 fmol of labeled probe and increasing concentrations of HpFur protein (from 3.4 to 112 nM of the apo-HpFur dimer and 1.7 to 56 nM

of the holo-HpFur tetramer) in HpFur footprinting buffer 1X (10 mM Tris-Cl, pH 7.85, 50 mM NaCl, 10 mM KCl, 0.02% Igepal CA-630, 10% glycerol; all from Merck), with 300 ng of salmon sperm DNA (Invitrogen) as a nonspecific competitor, either 150 μM $(NH_4)_2Fe(SO_4)_2$ (fe+) or 150 μM 2,2′-Dipyridyl (fe−), and 5 mM DTT to maintain Fe(II) in a reduced state, in a final volume of 50 μL. After an incubation for 15 min at room temperature, DNaseI (0.03 U for fe+ condition, 0.15 U for fe− condition; Novagen) diluted in footprinting buffer containing 10 mM $CaCl_2$ and 5 mM $MgCl_2$ was added to the reaction mixture (2 μl) and digestion was allowed to occur for 90 s. The reaction was stopped, purified and resuspended in formamide loading buffer; samples were denatured at 100 °C for 3 min, separated on 8 M urea–6% acrylamide sequencing gels in TBE buffer and autoradiographed; a modified G + A sequencing ladder protocol was employed to map the binding sites, according to.[46]

EMSA assay. DNA fragments encompassing the indicated promoter regions were amplified on *H. pylori* genomic DNA with the oligonucleotides reported in Supplementary Table 7: *ansB* (ansb_EMSA_F, ansb_EMSA_R) *vlpC* (vlpc_EMSA_F, vlpc_EMSA_R), *rs05875* (5875_EMSA_F, 5875_EMSA_R), *dld* (dld_EMSA_F, dld_EMSA_R), and 16S control (16S-RTF, 16S-RTR). The *rs03705* and *rs03705*ΔFurBS probes were amplified with oligos 761_Bam_R and VSLuxC2 on G27 (P*rs03705-lux*) and G27 (P*rs03705-lux*ΔFurBS) strains, respectively. Approximately 4 nM of the DNA probe were incubated with increasing concentrations of HpFur in EMSA buffer (10 mM Tris pH 8.0, 50 mM NaCl, 10 mM KCl, 0.01% NP-40, 10% glycerol) in presence of a > 30-fold excess of a plasmid vector (pBluescript II KS minus linearized with XbaI) as non-specific DNA competitor, 2 μg of BSA (Merck), and 5 mM DTT to maintain Fe(II) in a reduced state, in a final volume of 20 μL. The buffer was supplemented either with 150 μM $(NH_4)_2Fe(SO_4)_2{\cdot}6H_2O$ or 150 μM 2,2′-dipyridyl. Binding reactions were incubated at 25 °C for 15 min and resolved on native 6% polyacrylamide [19:1] gel (Thermo Fisher) in 0.5X Tris-borate (TB) buffer (30 mM Tris, 120 mM boric acid, pH 8.0; Merck). The gels were pre-run at 90 V for 30 min prior to loading and then run at 110 V for 1 h at room temperature. Gels were stained with Ethidium Bromide (1 μg/ml; Merck), and visualized on a ChemiDoc™ MP Imaging System (BioRad). For RNApol-HpFur interference assay, 4 nM of target DNA were incubated with the indicated amounts of *E. coli* RNApol holoenzyme (NEB) in modified RNApol reaction buffer (40 mM Tris-HCl pH 7.5, 150 mM KCl, 10 mM $MgCl_2$, 5 mM DTT, 0.01% NP-40), in presence of > 30-fold excess of a plasmid vector, 2 μg BSA, and 150 μM 2,2′-dipyridyl, in a final volume of 10 μL. Binding reactions were incubated at 37 °C for 10 min, then HpFur protein was added (final volume 12 μL) and incubated at 37 °C for 20 min. Samples were resolved on native 0.5X TB, 2% agarose gel, which was pre-run at 90 V for 30 min prior to loading and then run at 110 V for 90 min at room temperature. Gel was stained and visualized as described above.

In vitro transcription. About 800 ng of the *rs03705* or *rs03705*ΔFurBS probes were incubated with the indicated amounts of *E. coli* RNApol holoenzyme in the modified RNApol reaction buffer, with the addition of 2 μg BSA and 150 μM 2,2′-dipyridyl, in a final volume of 12 μL. Binding reactions were incubated at 37 °C for 10 min, then HpFur protein was added (final volume 14 μL) and the samples were incubated at 37 °C for 20 min. Two μL NTPs mix (5 mM each, Thermo Fisher) were added to start in vitro transcription and the reaction was stopped after 10 min by the addition of 16 μL 2 M NaCl. 100 ng of total RNA purified from G27 wild type (*luxC*-negative) strain was added to each sample for internal control. RNA was purified as described, and one-fifth of the sample was employed for DNA removal (two rounds), cDNA synthesis, and qRT-PCR analysis.

Consensus sequence analysis and other bioinformatic analyses. The newly validated HpFur promotorial binding sites as well as the previously individuated ones were used as input for consensus analysis. We adopted the GLAM2 tool which is specialized in finding gapped motifs to individuate HpFur binding sequence. The output was generated using default parameters. Protein signal peptide was predicted by SignalP 4.1 Server (https://www.cbs.dtu.dk/services/SignalP/). Protein transmembrane domains were predicted by TMHMM Server v. 2.0 (https://www.cbs.dtu.dk/services/TMHMM/). Protein tertiary structures were predicted by Phyre2 (https://www.sbg.bio.ic.ac.uk/phyre2/).

CRediT authorship contribution statement

Andrea Vannini: Writing – original draft, Visualization, Methodology, Investigation, Data curation, Conceptualization. **Eva Pinatel:** Writing – original draft, Software, Methodology, Investigation, Data curation, Conceptualization. **Paolo Emidio Costantini:** Writing – review & editing, Investigation. **Simone Pelliciari:** Writing – review & editing, Methodology, Investigation. **Davide Roncarati:** Writing – review & editing, Investigation. **Simone Puccio:** Writing – review & editing, Software, Methodology, Investigation. **Gianluca De Bellis:** Writing – review & editing, Supervision, Conceptualization. **Vincenzo Scarlato:** Writing – review & editing, Supervision, Funding acquisition, Conceptualization. **Clelia Peano:** Writing – review & editing, Project administration, Methodology, Investigation, Funding acquisition, Conceptualization. **Alberto**

Danielli: Writing – review & editing, Supervision, Project administration, Methodology, Funding acquisition, Conceptualization.

DATA AVAILABILITY

Bam files are publicly available at Sequence Reads Archive (SRA) under accession number BioProject PRJNA313048

DECLARATION OF COMPETING INTEREST

The authors declare that they have no known competing financial interests or personal relationships that could have appeared to influence the work reported in this paper.

Acknowledgements

This work was supported by Grants from the Italian Ministry of Education and University to VS (2020YXFSW5 and 2010P3S8BR_003), to CP (2010P3S8BR_002), and from grants by the University of Bologna to AD, AV, DR, and VS.

Appendix A. Supplementary data

Supplementary data to this article can be found online at https://doi.org/10.1016/j.jmb.2024.168573.

Received 13 December 2023;
Accepted 10 April 2024;
Available online 16 April 2024

Keywords:
Fur;
HpFur;
Helicobacter pylori;
regulation of transcription;
environmental response

† Equally contributed.

References

1. Benoit, S.L., Maier, R.J., Sawers, R.G., Greening, C., (2020). Molecular hydrogen metabolism: a widespread trait of pathogenic bacteria and protists. *Microbiol. Mol. Biol. Rev.* **84**, https://doi.org/10.1128/MMBR.00092-19 e00092-19.
2. Macomber, L., Hausinger, R.P., (2011). Mechanisms of nickel toxicity in microorganisms. *Metallomics* **3**, 1153. https://doi.org/10.1039/c1mt00063b.
3. Bereswill, S., Lichte, F., Vey, T., Fassbinder, F., Kist, M., (1998). Cloning and characterization of the *fur* gene from *Helicobacter pylori*. *FEMS Microbiol. Letter* **159**, 193–200. https://doi.org/10.1111/j.1574-6968.1998.tb12860.x.
4. Pich, O.Q., Merrell, D.S., (2013). The ferric uptake regulator of Helicobacter pylori : a critical player in the battle for iron and colonization of the stomach. *Future Microbiol.* **8**, 725–738. https://doi.org/10.2217/fmb.13.43.
5. Vannini, A., Roncarati, D., D'Agostino, F., Antoniciello, F., Scarlato, V., (2022). Insights into the orchestration of gene transcription regulators in helicobacter pylori. *IJMS* **23**, 13688. https://doi.org/10.3390/ijms232213688.
6. Bagg, A., Neilands, J.B., (1987). Ferric uptake regulation protein acts as a repressor, employing iron(II) as a cofactor to bind the operator of an iron transport operon in Escherichia coli. *Biochemistry* **26**, 5471–5477. https://doi.org/10.1021/bi00391a039.
7. Troxell, B., Hassan, H.M., (2013). Transcriptional regulation by Ferric Uptake Regulator (Fur) in pathogenic bacteria. *Front. Cell. Infect. Microbiol.* **3** https://doi.org/10.3389/fcimb.2013.00059.
8. Baichoo, N., Helmann, J.D., (2002). Recognition of DNA by Fur: a reinterpretation of the fur box consensus sequence. *J. Bacteriol.* **184**, 5826–5832. https://doi.org/10.1128/JB.184.21.5826-5832.2002.
9. Massé, E., Gottesman, S., (2002). A small RNA regulates the expression of genes involved in iron metabolism in *Escherichia coli*. *PNAS* **99**, 4620–4625. https://doi.org/10.1073/pnas.032066599.
10. Metruccio, M.M.E., Fantappiè, L., Serruto, D., Muzzi, A., Roncarati, D., Donati, C., Scarlato, V., Delany, I., (2009). The Hfq-dependent small noncoding RNA NrrF directly mediates fur-dependent positive regulation of succinate dehydrogenase in *Neisseria meningitidis*. *J. Bacteriol.* **191**, 1330–1342. https://doi.org/10.1128/JB.00849-08.
11. Oglesby-Sherrouse, A.G., Murphy, E.R., (2013). Iron-responsive bacterial small RNAs: variations on a theme. *Metallomics* **5**, 276. https://doi.org/10.1039/c3mt20224k.
12. Nandal, A., Huggins, C.C.O., Woodhall, M.R., McHugh, J., Rodríguez-Quiñones, F., Quail, M.A., Guest, J.R., Andrews, S.C., (2010). Induction of the ferritin gene (ftnA) of Escherichia coli by Fe 2+ –Fur is mediated by reversal of H-NS silencing and is RyhB independent. *Mol. Microbiol.* **75**, 637–657. https://doi.org/10.1111/j.1365-2958.2009.06977.x.
13. Pinochet-Barros, A., Helmann, J.D., (2020). Bacillus subtilis fur is a transcriptional activator for the PerR-Repressed *pfeT* gene, encoding an iron efflux pump. *J. Bacteriol.* **202** https://doi.org/10.1128/JB.00697-19.
14. Delany, I., Rappuoli, R., Scarlato, V., (2004). Fur functions as an activator and as a repressor of putative virulence genes in *Neisseria meningitidis*. *Mol. Microbiol.* **52**, 1081–1090. https://doi.org/10.1111/j.1365-2958.2004.04030.x.
15. Teixidó, L., Carrasco, B., Alonso, J.C., Barbé, J., Campoy, S., (2011). Fur activates the expression of salmonella enterica pathogenicity island 1 by directly interacting with the hilD operator in vivo and in vitro. *PLoS One* **6**, e19711. https://doi.org/10.1371/journal.pone.0019711.
16. Craig, S.A., Carpenter, C.D., Mey, A.R., Wyckoff, E.E., Payne, S.M., (2011). Positive regulation of the vibrio cholerae porin OmpT by iron and fur. *J. Bacteriol.* **193**, 6505–6511. https://doi.org/10.1128/JB.05681-11.
17. Seo, S.W., Kim, D., Latif, H., O'Brien, E.J., Szubin, R., Palsson, B.O., (2014). Deciphering Fur transcriptional regulatory network highlights its complex role beyond iron metabolism in Escherichia coli. *Nature Commun.* **5**, 4910. https://doi.org/10.1038/ncomms5910.
18. Gao, H., Ma, L., Qin, Q., Qiu, Y., Zhang, J., Li, J., Lou, J., Diao, B., Zhao, H., Shi, Q., Zhang, Y., Kan, B., (2020). Fur

represses vibrio cholerae biofilm formation via direct regulation of vieSAB, cdgD, vpsU, and vpsA-K transcription. *Front. Microbiol.* **11**, https://doi.org/10.3389/fmicb.2020.587159 587159.
19. Steingard, C.H., Helmann, J.D., (2023). Meddling with metal sensors: fur-family proteins as signaling hubs e00022-23 *J. Bacteriol.* **205** https://doi.org/10.1128/jb.00022-23.
20. Deng, X., Sun, F., Ji, Q., Liang, H., Missiakas, D., Lan, L., He, C., (2012). Expression of multidrug resistance efflux pump gene *norA* is iron responsive in Staphylococcus aureus. *J. Bacteriol.* **194**, 1753–1762. https://doi.org/10.1128/JB.06582-11.
21. Grabowska, A.D., Wandel, M.P., Łasica, A.M., Nesteruk, M., Roszczenko, P., Wyszyńska, A., Godlewska, R., Jagusztyn-Krynicka, E.K., (2011). Campylobacter jejuni dsb gene expression is regulated by iron in a Fur-dependent manner and by a translational coupling mechanism. *BMC Microbiol.* **11**, 166. https://doi.org/10.1186/1471-2180-11-166.
22. Sarvan, S., Charih, F., Askoura, M., Butcher, J., Brunzelle, J.S., Stintzi, A., Couture, J.-F., (2018). Functional insights into the interplay between DNA interaction and metal coordination in ferric uptake regulators. *Sci. Rep.* **8**, 7140. https://doi.org/10.1038/s41598-018-25157-6.
23. Gilbreath, J.J., West, A.L., Pich, O.Q., Carpenter, B.M., Michel, S., Merrell, D.S., (2012). Fur activates expression of the 2-oxoglutarate oxidoreductase genes (oorDABC) in Helicobacter pylori. *J. Bacteriol.* **194**, 6490–6497. https://doi.org/10.1128/JB.01226-12.
24. Butcher, J., Sarvan, S., Brunzelle, J.S., Couture, J.-F., Stintzi, A., (2012). Structure and regulon of *Campylobacter jejuni* ferric uptake regulator Fur define apo-Fur regulation. *PNAS* **109**, 10047–10052. https://doi.org/10.1073/pnas.1118321109.
25. Dian, C., Vitale, S., Leonard, G.A., Bahlawane, C., Fauquant, C., Leduc, D., Muller, C., de Reuse, H., Michaud-Soret, I., Terradot, L., (2011). The structure of the Helicobacter pylori ferric uptake regulator Fur reveals three functional metal binding sites: crystal structure of Fur from Helicobacter pylori. *Mol. Microbiol.* **79**, 1260–1275. https://doi.org/10.1111/j.1365-2958.2010.07517.x.
26. Gilbreath, J.J., Pich, O.Q., Benoit, S.L., Besold, A.N., Cha, J.-H., Maier, R.J., Michel, S.L.J., Maynard, E.L., Merrell, D. S., (2013). Random and site-specific mutagenesis of the *Helicobacter pylori* ferric uptake regulator provides insight into Fur structure-function relationships: *H. pylori* Fur mutagenesis. *Mol. Microbiol.* **89**, 304–323. https://doi.org/10.1111/mmi.12278.
27. Agriesti, F., Roncarati, D., Musiani, F., Del Campo, C., Iurlaro, M., Sparla, F., Ciurli, S., Danielli, A., Scarlato, V., (2014). FeON-FeOFF: the Helicobacter pylori Fur regulator commutates iron-responsive transcription by discriminative readout of opposed DNA grooves. *Nucleic Acids Res.* **42**, 3138–3151. https://doi.org/10.1093/nar/gkt1258.
28. Danielli, A., Roncarati, D., Delany, I., Chiarini, V., Rappuoli, R., Scarlato, V., (2006). In vivo dissection of the *Helicobacter pylori* fur regulatory circuit by genome-wide location analysis. *J. Bacteriol.* **188**, 4654–4662. https://doi.org/10.1128/JB.00120-06.
29. Pich, O.Q., Carpenter, B.M., Gilbreath, J.J., Merrell, D.S., (2012). Detailed analysis of Helicobacter pylori Fur-regulated promoters reveals a Fur box core sequence and novel Fur-regulated genes: The Fur box of H. pylori. *Mol. Microbiol.* **84**, 921–941. https://doi.org/10.1111/j.1365-2958.2012.08066.x.
30. Bereswill, S., Greiner, S., van Vliet, A.H.M., Waidner, B., Fassbinder, F., Schiltz, E., Kusters, J.G., Kist, M., (2000). Regulation of ferritin-mediated cytoplasmic iron storage by the ferric uptake regulator homolog (Fur) of Helicobacter pylori. *J. Bacteriol.* **182**, 5948–5953. https://doi.org/10.1128/JB.182.21.5948-5953.2000.
31. Delany, I., Spohn, G., Rappuoli, R., Scarlato, V., (2002). The Fur repressor controls transcription of iron-activated and -repressed genes in Helicobacter pylori: iron regulation in H. pylori. *Mol. Microbiol.* **42**, 1297–1309. https://doi.org/10.1046/j.1365-2958.2001.02696.x.
32. Ernst, F.D., Homuth, G., Stoof, J., Mäder, U., Waidner, B., Kuipers, E.J., Kist, M., Kusters, J.G., Bereswill, S., van Vliet, A.H.M., (2005). Iron-responsive regulation of the *Helicobacter pylori* iron-cofactored superoxide dismutase sodb is mediated by Fur. *J. Bacteriol.* **187**, 3687–3692. https://doi.org/10.1128/JB.187.11.3687-3692.2005.
33. Gancz, H., Censini, S., Merrell, D.S., (2006). Iron and pH homeostasis intersect at the level of fur regulation in the gastric pathogen *Helicobacter pylori*. *Infect. Immun.* **74**, 602–614. https://doi.org/10.1128/IAI.74.1.602-614.2006.
34. Carpenter, B.M., Gilbreath, J.J., Pich, O.Q., McKelvey, A. M., Maynard, E.L., Li, Z.-Z., Merrell, D.S., (2013). Identification and characterization of novel helicobacter pylori apo-fur-regulated target genes. *J. Bacteriol.* **195**, 5526–5539. https://doi.org/10.1128/JB.01026-13.
35. Vannini, A., Roncarati, D., Spinsanti, M., Scarlato, V., Danielli, A., (2014). In depth analysis of the helicobacter pylori cag pathogenicity island transcriptional responses. *PLoS One* **9**, e98416. https://doi.org/10.1371/journal.pone.0098416.
36. Delany, I., Spohn, G., Pacheco, A.-B.-F., Ieva, R., Alaimo, C., Rappuoli, R., Scarlato, V., (2002). Autoregulation of Helicobacter pylori Fur revealed by functional analysis of the iron-binding site: Autoregulation of H. pylori Fur protein. *Mol. Microbiol.* **46**, 1107–1122. https://doi.org/10.1046/j.1365-2958.2002.03227.x.
37. Delany, I., Ieva, R., Alaimo, C., Rappuoli, R., Scarlato, V., (2003). The iron-responsive regulator fur is transcriptionally autoregulated and not essential in *Neisseria meningitidis*. *J. Bacteriol.* **185**, 6032–6041. https://doi.org/10.1128/JB.185.20.6032-6041.2003.
38. Pflock, M., Kennard, S., Delany, I., Scarlato, V., Beier, D., (2005). Acid-induced activation of the urease promoters is mediated directly by the ArsRS two-component system of *Helicobacter pylori*. *Infect. Immun.* **73**, 6437–6445. https://doi.org/10.1128/IAI.73.10.6437-6445.2005.
39. Roncarati, D., Pelliciari, S., Doniselli, N., Maggi, S., Vannini, A., Valzania, L., Mazzei, L., Zambelli, B., Rivetti, C., Danielli, A., (2016). Metal-responsive promoter DNA compaction by the ferric uptake regulator. *Nature Commun.* **7**, 12593. https://doi.org/10.1038/ncomms12593.
40. Delany, I., Pacheco, A.B.F., Spohn, G., Rappuoli, R., Scarlato, V., (2001). Iron-dependent transcription of the *frpB* Gene of *Helicobacter pylori* is controlled by the fur repressor protein. *J. Bacteriol.* **183**, 4932–4937. https://doi.org/10.1128/JB.183.16.4932-4937.2001.
41. Danielli, A., Romagnoli, S., Roncarati, D., Costantino, L., Delany, I., Scarlato, V., (2009). Growth phase and metal-dependent transcriptional regulation of the *fecA* Genes in

Helicobacter pylori. *J. Bacteriol.* **191**, 3717–3725. https://doi.org/10.1128/JB.01741-08.
42. van Vliet, A.H.M., Stoof, J., Poppelaars, S.W., Bereswill, S., Homuth, G., Kist, M., Kuipers, E.J., Kusters, J.G., (2003). Differential regulation of amidase- and formamidase-mediated ammonia production by the helicobacter pylori fur repressor. *J. Biol. Chem.* **278**, 9052–9057. https://doi.org/10.1074/jbc.M207542200.
43. Ernst, F.D., Bereswill, S., Waidner, B., Stoof, J., Mäder, U., Kusters, J.G., Kuipers, E.J., Kist, M., van Vliet, A.H.M., Homuth, G., (2005). Transcriptional profiling of Helicobacter pylori Fur- and iron-regulated gene expression. *Microbiology* **151**, 533–546. https://doi.org/10.1099/mic.0.27404-0.
44. Alamuri, P., Mehta, N., Burk, A., Maier, R.J., (2006). Regulation of the *Helicobacter pylori* Fe-S cluster synthesis protein NifS by iron, oxidative stress conditions, and fur. *J. Bacteriol.* **188**, 5325–5330. https://doi.org/10.1128/JB.00104-06.
45. Merrell, D.S., Thompson, L.J., Kim, C.C., Mitchell, H., Tompkins, L.S., Lee, A., Falkow, S., (2003). Growth phase-dependent response of *Helicobacter pylori* to iron starvation. *Infect. Immun.* **71**, 6510–6525. https://doi.org/10.1128/IAI.71.11.6510-6525.2003.
46. Pelliciari, S., Vannini, A., Roncarati, D., Danielli, A., (2015). The allosteric behavior of Fur mediates oxidative stress signal transduction in Helicobacter pylori. *Front. Microbiol.* **6** https://doi.org/10.3389/fmicb.2015.00840.
47. Delany, I., Ieva, R., Soragni, A., Hilleringmann, M., Rappuoli, R., Scarlato, V., (2005). In vitro analysis of protein-operator interactions of the NikR and fur metal-responsive regulators of coregulated genes in *Helicobacter pylori*. *J. Bacteriol.* **187**, 7703–7715. https://doi.org/10.1128/JB.187.22.7703-7715.2005.
48. Sharma, C.M., Hoffmann, S., Darfeuille, F., Reignier, J., Findeiß, S., Sittka, A., Chabas, S., Reiche, K., Hackermüller, J., Reinhardt, R., Stadler, P.F., Vogel, J., (2010). The primary transcriptome of the major human pathogen Helicobacter pylori. *Nature* **464**, 250–255. https://doi.org/10.1038/nature08756.
49. Danielli, A., Amore, G., Scarlato, V., (2010). Built shallow to maintain homeostasis and persistent infection: insight into the transcriptional regulatory network of the gastric human pathogen Helicobacter pylori. *PLoS Pathog.* **6**, e1000938. https://doi.org/10.1371/journal.ppat.1000938.
50. Vannini, A., Pinatel, E., Costantini, P.E., Pelliciari, S., Roncarati, D., Puccio, S., De Bellis, G., Peano, C., Danielli, A., (2017). Comprehensive mapping of the Helicobacter pylori NikR regulon provides new insights in bacterial nickel responses. *Sci. Rep.* **7**, 45458. https://doi.org/10.1038/srep45458.
51. Pelliciari, S., Pinatel, E., Vannini, A., Peano, C., Puccio, S., De Bellis, G., Danielli, A., Scarlato, V., Roncarati, D., (2017). Insight into the essential role of the Helicobacter pylori HP1043 orphan response regulator: genome-wide identification and characterization of the DNA-binding sites. *Sci. Rep.* **7**, 41063. https://doi.org/10.1038/srep41063.
52. Butcher, B.G., Bronstein, P.A., Myers, C.R., Stodghill, P.V., Bolton, J.J., Markel, E.J., Filiatrault, M.J., Swingle, B., Gaballa, A., Helmann, J.D., (2011). Characterization of the Fur regulon in Pseudomonas syringae pv. tomato DC3000. *J. Bacteriol.* **193**, 4598–4611.
53. Pi, H., Helmann, J.D., (2018). Genome-wide characterization of the Fur regulatory network reveals a link between catechol degradation and bacillibactin metabolism in Bacillus subtilis. *MBio* **9** https://doi.org/10.1128/mbio. 01451-18.
54. Shoyama, F.M., Janetanakit, T., Bannantine, J.P., Barletta, R.G., Sreevatsan, S., (2020). Elucidating the regulon of a fur-like protein in mycobacterium avium subsp. paratuberculosis (MAP). *Front. Microbiol.* **11**, 598.
55. Visweswariah, S.S., Busby, S.J.W., (2015). Evolution of bacterial transcription factors: how proteins take on new tasks, but do not always stop doing the old ones. *Trends Microbiol.* **23**, 463–467. https://doi.org/10.1016/j.tim.2015.04.009.
56. Fassbinder, F., Vliet, A.H.M., Gimmel, V., Kusters, J.G., Kist, M., Bereswill, S., (2000). Identification of iron-regulated genes of Helicobacter pylori by a modified Fur titration assay (FURTA-Hp). *FEMS Microbiol. Letter* **184**, 225–229. https://doi.org/10.1111/j.1574-6968.2000.tb09018.x.
57. Worst, D.J., Gerrits, M.M., Vandenbroucke-Grauls, C.M.J. E., Kusters, J.G., (1998). *Helicobacter pylori ribBA* - mediated riboflavin production is involved in iron acquisition. *J. Bacteriol.* **180**, 1473–1479. https://doi.org/10.1128/JB.180.6.1473-1479.1998.
58. Bereswill, S., Fassbinder, F., Völzing, C., Covacci, A., Haas, R., Kist, M., (1998). Hemolytic properties and riboflavin synthesis of Helicobacter pylori: cloning and functional characterization of the rib A gene encoding GTP-cyclohydrolase II that confers hemolytic activity to Escherichia coli. *Med. Microbiol. Immunol.* **186**, 177–187. https://doi.org/10.1007/s004300050062.
59. Bantysh, O., Serebryakova, M., Makarova, K.S., Dubiley, S., Datsenko, K.A., Severinov, K., (2014). Enzymatic synthesis of bioinformatically predicted microcin C-Like compounds encoded by diverse bacteria e01059-14 *MBio* **5** https://doi.org/10.1128/mBio.01059-14.
60. Singh, G., Yadav, M., Ghosh, C., Rathore, J.S., (2021). Bacterial toxin-antitoxin modules: classification, functions, and association with persistence. *Curr. Res. Microb. Sci.* **2**, https://doi.org/10.1016/j.crmicr.2021.100047 100047.
61. Marcus, E.A., Sachs, G., Scott, D.R., (2018). Acid-regulated gene expression of Helicobacter pylori: insight into acid protection and gastric colonization. *Helicobacter* **23**, e12490. https://doi.org/10.1111/hel.12490.
62. Bereswill, S., Waidner, U., Odenbreit, S., Lichte, F., Fassbinder, F., Bode, G., Kist, M., (1998). Structural, functional and mutational analysis of the pfr gene encoding a ferritin from Helicobacter pylori. *Microbiology* **144**, 2505–2516. https://doi.org/10.1099/00221287-144-9-2505.
63. Pinske, C., Sawers, R.G., (2014). The importance of iron in the biosynthesis and assembly of [NiFe]-hydrogenases. *Biomol. Concepts* **5**, 55–70. https://doi.org/10.1515/bmc-2014-0001.
64. Koyanagi, S., Nagata, K., Tamura, T., Tsukita, S., Sone, N., (2000). Purification and characterization of cytochrome c-553 from Helicobacter pylori. *J. Biochem.* **128**, 371–375. https://doi.org/10.1093/oxfordjournals.jbchem.a022763.
65. Benoit, S.L., Holland, A.A., Johnson, M.K., Maier, R.J., (2018). Iron-sulfur protein maturation in Helicobacter pylori : identifying a Nfu-type cluster carrier protein and its iron-sulfur protein targets: Iron-sulfur cluster maturation in H. pylori. *Mol. Microbiol.* **108**, 379–396. https://doi.org/10.1111/mmi.13942.

66. Sun, H.-Y., Lin, S.-W., Ko, T.-P., Pan, J.-F., Liu, C.-L., Lin, C.-N., Wang, A.-H.-J., Lin, C.-H., (2007). Structure and Mechanism of Helicobacter pylori Fucosyltransferase. *J. Biol. Chem.* **282**, 9973–9982. https://doi.org/10.1074/jbc.M610285200.
67. Cheng, J., Liu, W.-Q., Zhu, X., Zhang, Q., (2022). Functional diversity of HemN-like proteins. *ACS Bio. Med. Chem. Au.* **2**, 109–119. https://doi.org/10.1021/acsbiomedchemau.1c00058.
68. Wang, G., Maier, R.J., (2004). An NADPH quinone reductase of *Helicobacter pylori* plays an important role in oxidative stress resistance and host colonization. *Infect. Immun.* **72**, 1391–1396. https://doi.org/10.1128/IAI.72.3.1391-1396.2004.
69. Sutherland, M.C., Mendez, D.L., Babbitt, S.E., Tillman, D. E., Melnikov, O., Tran, N.L., Prizant, N.T., Collier, A.L., Kranz, R.G., (2021). In vitro reconstitution reveals major differences between human and bacterial cytochrome c synthases. *Elife* **10**, e64891. https://doi.org/10.7554/eLife.64891.
70. Kim, A., Servetas, S.L., Kang, J., Kim, J., Jang, S., Choi, Y. H., Su, H., Jeon, Y.-E., Hong, Y.A., Yoo, Y.-J., Merrell, D. S., Cha, J.-H., (2016). Helicobacter pylori outer membrane protein, HomC, shows geographic dependent polymorphism that is influenced by the Bab family. *J. Microbiol.* **54**, 846–852. https://doi.org/10.1007/s12275-016-6434-8.
71. Foegeding, N., Caston, R., McClain, M., Ohi, M., Cover, T., (2016). An overview of Helicobacter pylori VacA toxin biology. *Toxins* **8**, 173. https://doi.org/10.3390/toxins8060173.
72. Falsafi, T., Ehsani, A., Attaran, B., Niknam, V., (2016). Association of hp1181 and hp1184 genes with the active efflux phenotype in multidrug-resistant isolates of Helicobacter pylori. *Jundishapur J. Microbiol.* **9** https://doi.org/10.5812/jjm.30726.
73. Leduc, D., Gallaud, J., Stingl, K., de Reuse, H., (2010). Coupled amino acid deamidase-transport systems essential for *Helicobacter pylori* colonization. *Infect. Immun.* **78**, 2782–2792. https://doi.org/10.1128/IAI.00149-10.
74. Langmead, B., Salzberg, S.L., (2012). Fast gapped-read alignment with Bowtie 2. *Nature Methods* **9**, 357–359. https://doi.org/10.1038/nmeth.1923.
75. Pepe, S., Pinatel, E., Fiore, E., Puccio, S., Peano, C., Brignoli, T., Vannini, A., Danielli, A., Scarlato, V., Roncarati, D., (2018). The Helicobacter pylori heat-shock repressor HspR: definition of its direct regulon and characterization of the cooperative DNA-binding mechanism on its own promoter. *Front. Microbiol.* **9**, 1887. https://doi.org/10.3389/fmicb.2018.01887.
76. Quinlan, A.R., Hall, I.M., (2010). BEDTools: a flexible suite of utilities for comparing genomic features. *Bioinformatics* **26**, 841–842. https://doi.org/10.1093/bioinformatics/btq033.
77. Li, H., Handsaker, B., Wysoker, A., Fennell, T., Ruan, J., Homer, N., Marth, G., Abecasis, G., Durbin, R., (2009). 1000 genome project data processing subgroup, the sequence alignment/map format and SAMtools. *Bioinformatics* **25**, 2078–2079. https://doi.org/10.1093/bioinformatics/btp352.
78. Pinatel, E., Peano, C., (2018). RNA sequencing and analysis in microorganisms for metabolic network reconstruction. In: Fondi, M. (Ed.), *Metabolic Network Reconstruction and Modeling*. Springer New York, New York, NY, pp. 239–265 https://doi.org/10.1007/978-1-4939-7528-0_11.
79. Love, M.I., Huber, W., Anders, S., (2014). Moderated estimation of fold change and dispersion for RNA-seq data with DESeq2. *Genome Biol.* **15**, 550. https://doi.org/10.1186/s13059-014-0550-8.
80. Li, Q., Brown, J.B., Huang, H., Bickel, P.J., (2011). Measuring reproducibility of high-throughput experiments. *Ann. Appl. Stat.*. https://doi.org/10.48550/ARXIV.1110.4705.
81. Heinz, S., Benner, C., Spann, N., Bertolino, E., Lin, Y.C., Laslo, P., Cheng, J.X., Murre, C., Singh, H., Glass, C.K., (2010). Simple combinations of lineage-determining transcription factors prime cis-regulatory elements required for macrophage and B cell identities. *Mol. Cell* **38**, 576–589. https://doi.org/10.1016/j.molcel.2010.05.004.